

Article

## DDX3X helicase inhibitors as new strategy to fight West Nile Virus infection

Annalaura Brai, Francesco Martelli, Valentina Riva, Anna Garbelli, Roberta Fazi, Claudio Zamperini, Alessandro Pollutri, Lucia Falsitta, Stefania Ronzini, Laura Maccari, Giovanni Maga, Simone Giannecchini, and Maurizio Botta

*J. Med. Chem.*, **Just Accepted Manuscript** • DOI: 10.1021/acs.jmedchem.8b01403 • Publication Date (Web): 05 Feb 2019

Downloaded from <http://pubs.acs.org> on February 6, 2019

### Just Accepted

“Just Accepted” manuscripts have been peer-reviewed and accepted for publication. They are posted online prior to technical editing, formatting for publication and author proofing. The American Chemical Society provides “Just Accepted” as a service to the research community to expedite the dissemination of scientific material as soon as possible after acceptance. “Just Accepted” manuscripts appear in full in PDF format accompanied by an HTML abstract. “Just Accepted” manuscripts have been fully peer reviewed, but should not be considered the official version of record. They are citable by the Digital Object Identifier (DOI®). “Just Accepted” is an optional service offered to authors. Therefore, the “Just Accepted” Web site may not include all articles that will be published in the journal. After a manuscript is technically edited and formatted, it will be removed from the “Just Accepted” Web site and published as an ASAP article. Note that technical editing may introduce minor changes to the manuscript text and/or graphics which could affect content, and all legal disclaimers and ethical guidelines that apply to the journal pertain. ACS cannot be held responsible for errors or consequences arising from the use of information contained in these “Just Accepted” manuscripts.

# DDX3X helicase inhibitors as new strategy to fight West Nile Virus infection

*Annalaura Brai,<sup>1,2</sup> Francesco Martelli,<sup>3</sup> Valentina Riva,<sup>4</sup> Anna Garbelli,<sup>4</sup> Roberta Fazi,<sup>1</sup>*

*Claudio Zamperini,<sup>1,2</sup> Alessandro Pollutri,<sup>1</sup> Lucia Falsitta,<sup>1</sup> Stefania Ronzini,<sup>1</sup> Laura*

*Maccari,<sup>2</sup> Giovanni Maga,<sup>4</sup> Simone Giannecchini<sup>3</sup> and Maurizio Botta<sup>1,2,5,\*</sup>*

<sup>1</sup>Dipartimento Biotecnologie, Chimica e Farmacia, Università degli Studi di Siena, Via A.

De Gasperi 2, I-53100 Siena, Italy. <sup>2</sup> Lead Discovery Siena S.r.l., Castelnuovo

Berardenga, I-53019 Siena, Italy. <sup>3</sup>Department of Experimental and Clinical Medicine,

University of Florence, I-50134 Florence, Italy. <sup>4</sup>Istituto di Genetica Molecolare, IGM-

CNR, Via Abbiategrasso 207, I-27100 Pavia, Italy. <sup>5</sup>Biotechnology College of Science

and Technology, Temple University, Biolife Science Building, Suite 333, 1900 N 12<sup>th</sup>

Street, Philadelphia, Pennsylvania 19122.

1  
2  
3  
4 KEYWORDS: DDX3X • antivirals • West Nile Virus• arbovirus • host factors  
5  
6  
7  
8  
9  
10  
11  
12  
13  
14  
15  
16  
17  
18  
19  
20  
21  
22  
23  
24  
25  
26  
27  
28  
29  
30  
31  
32  
33  
34  
35  
36  
37  
38  
39  
40  
41  
42  
43  
44  
45  
46  
47  
48  
49  
50  
51  
52  
53  
54  
55  
56  
57  
58  
59  
60

1  
2  
3  
4  
5  
6  
7  
8  
9 ABSTRACT: Increased frequency of arbovirus outbreaks in the last ten years  
10  
11 represents an important emergence for global health. Climate warming, extensive  
12  
13 urbanization of tropical regions and human migrations flows facilitate the expansion of  
14  
15 anthropophilic mosquitos and the emerging or re-emerging of new viral infections. Only  
16  
17 recently the human ATPase/RNA helicase X-linked DEAD-box polypeptide 3 (DDX3X)  
18  
19 emerged as a novel therapeutic target in the fight against infectious diseases. Herein,  
20  
21 starting from our previous studies a new family of DDX3X inhibitors was designed,  
22  
23 synthesized, validated on the target enzyme and evaluated against West Nile Virus  
24  
25 (WNV) infection. Time of addition experiments after virus infection indicated that the  
26  
27 compounds exerted their antiviral activities after the entry process, likely at the protein  
28  
29 translation step of WNV replication. Finally, the most interesting compounds were then  
30  
31 analyzed for their *in vitro* pharmacokinetic parameters, revealing favorable ADME  
32  
33 values. The good safety profile together with a good activity against WNV for which no  
34  
35  
36  
37  
38  
39  
40  
41  
42  
43  
44  
45  
46  
47  
48  
49  
50  
51  
52  
53  
54  
55  
56  
57  
58  
59  
60

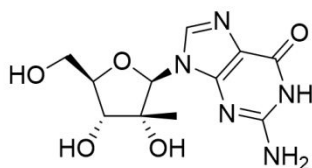
1  
2  
3  
4 treatments are currently available, make this new class of molecules a good starting  
5  
6  
7 point for further *in vivo* studies.  
8  
9  
10  
11  
12  
13  
14  
15  
16  
17  
18  
19  
20  
21  
22  
23  
24  
25  
26  
27  
28  
29  
30  
31  
32  
33  
34  
35  
36  
37  
38  
39  
40  
41  
42  
43  
44  
45  
46  
47  
48  
49  
50  
51  
52  
53  
54  
55  
56  
57  
58  
59  
60

## INTRODUCTION

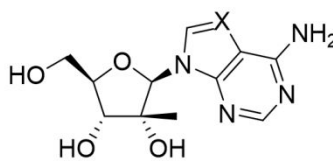
West Nile Virus (WNV) is a neurotropic arbovirus member of *Flaviviridae* family<sup>1</sup>. Since its introduction in Europe and America the number of novel infections is increasing, counting during 2017, 204 novel reported cases in Europe<sup>2</sup> and 2,002 in America<sup>3</sup>. The number is impressive considering that about 80% of WNV infections are usually asymptomatic and only the remaining 20% may cause meningitis, encephalitis or rarely in death 1%<sup>4</sup>. In addition, probably due to climate warming, the number of novel human cases sharply increased in EU member States during the current year, reaching 710 infections and 63 deaths as of 30 August.<sup>5</sup> The rapid diffusion of WNV is dependent on its zoonotic life cycle, that involves migratory birds, *Culex* and *Aedes* mosquitos and mammals including horses and humans. In this context inadequate vector control, globalization and human travel networks are only a few factors that are contributing to this and other arboviruses spread. Despite continuous efforts have been made to identify new drugs (Figure 1) or vaccines, no specific therapy or prophylaxis is actually available on the market and the treatment remains symptomatic<sup>6</sup>. In this

context, drug repurposing strategy provided new drug candidates to fight emerging and re-emerging viruses<sup>7</sup>, but often the antiviral compounds are poorly active or are direct on viral enzymes and are thus generally characterized by a low genetic barrier to resistance (Figure 1).

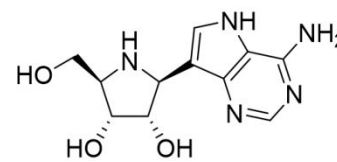
### RNA-DEPENDENT RNA POLYMERASE (RdRP) INHIBITORS



**2'-C-methylguanosine**  
 $EC_{50} = 30 \mu\text{M}$   $CC_{50} > 100 \mu\text{M}$

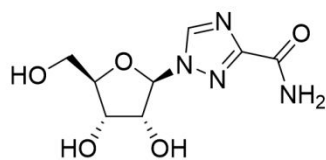


**2'-C-methyladenosine X=N**  
 $EC_{50} = 5.1 \mu\text{M}$   $CC_{50} = 25 \mu\text{M}$   
**7-Deaza-2'-C-methyl-adenosine X=CH**  
 $EC_{50} = 4.5 \mu\text{M}$   $CC_{50} = 250 \mu\text{M}$



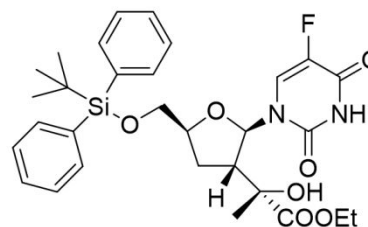
**BCX4430**  
 $EC_{50} = 2.33 \mu\text{M}$   $CC_{50} > 100 \mu\text{M}$

### MULTIPLE TARGETS



**Ribavirin**  
 $EC_{50} = 71.2 \mu\text{M}$   $CC_{50} > 100 \mu\text{M}$

### FLAVIVIRAL METHYLTRANSFERASE INHIBITOR



**GRL003**  
 $EC_{50} = 27 \mu\text{M}$   $CC_{50} = 236 \mu\text{M}$

**Figure 1.** 2D chemical structures of the known WNV inhibitors and their potential inhibitory target

1  
2  
3  
4 In the last years the human ATPase/RNA helicase X-linked DEAD-box polypeptide 3  
5  
6  
7 (DDX3X) protein has been identified as a component of critical host-cell pathways,  
8  
9  
10 hijacked by several pathogenic human viruses<sup>8</sup>. DDX3X is an ATP-dependent RNA  
11  
12  
13 helicase involved in many aspects of RNA metabolism such as transcription, translation  
14  
15  
16 and RNA decay. It localizes to P-bodies, cytoplasmic foci related to mRNA turnover  
17  
18  
19 which are disrupted in response to the infection of viruses such as WNV or Dengue  
20  
21  
22 virus (DENV)<sup>9</sup>. Furthermore, after WNV infection DDX3X was released from P-bodies  
23  
24  
25 and co-localized at a perinuclear region with viral NS3<sup>10</sup>. It was found, moreover, that  
26  
27  
28 DDX3X knockdown strongly decreased WNV replication, suggesting an important  
29  
30  
31 implication not yet completely understood<sup>10</sup>. Although its role in the life cycle of different  
32  
33  
34 viruses was extensively studied<sup>11-16</sup>, only few DDX3X inhibitors have been published as  
35  
36  
37 antiviral agents<sup>17-21</sup>, and the mechanism of action is clearly described only for HIV-1<sup>22</sup>.  
38  
39  
40  
41 In a recent work<sup>19</sup> we identified the first inhibitor of the helicase binding site of DDX3X  
42  
43  
44 also active against WNV. Such compound belonged to a family of DDX3X RNA-  
45  
46  
47  
48  
49  
50  
51  
52  
53  
54  
55  
56  
57  
58  
59  
60 *in vitro* and *in vivo* models. Among them, compound **16d** (compound **1** of the

1  
2  
3 manuscript), belonging to the urea series, was the first DDX3X inhibitor endowed with a  
4  
5  
6  
7 broad spectrum antiviral activity against HIV-1 (both wild-type and drug-resistant  
8  
9  
10 strains), HCV, and new emerging viruses (WNV and DENV)<sup>19</sup>. Despite **1** represented  
11  
12  
13 the proof of concept that DDX3X inhibitors could be used as novel antiviral drugs, its  
14  
15  
16 poor aqueous solubility limited its bioavailability in preclinical models causing its  
17  
18  
19 accumulation in fat tissues (LogS=-7.05).  
20  
21  
22  
23

24 With the attempt to enlarge our library of DDX3X inhibitors we performed a homology  
25  
26  
27 model-based virtual screening<sup>20</sup> that led us to identify another small molecule inhibitor of  
28  
29  
30 DDX3X helicase activity (compound **2** of the present paper) characterized by a  
31  
32  
33 sulfonamide moiety. Despite its low passive permeability, compound **2** was  
34  
35  
36 characterized by a very good aqueous solubility and at the same time by a promising  
37  
38  
39 anti-enzymatic activity value of 0.36  $\mu\text{M}^{20}$ . Pursuing our research of novel drug-like  
40  
41  
42 DDX3X inhibitors, we performed a docking analysis of the two hit compounds **1** and **2**.  
43  
44  
45  
46  
47  
48 On the basis of the 3D overlap of the two molecules within the binding site, we designed  
49  
50  
51 a new series of hybrid compounds by merging the key structural moieties of **1** and **2**  
52  
53  
54  
55  
56 able to interact with the main residues involved in the binding of both of them (Arg276,  
57  
58  
59  
60

1  
2  
3 Pro274 and Arg480). Novel compounds (**8-20** and **31-36** ) were then synthesized and  
4  
5  
6  
7 validated against DDX3X enzyme and evaluated for their ability to inhibit WNV  
8  
9  
10 replication, leading to a small library of derivatives endowed with antiviral activities  
11  
12  
13 comparable or higher than the broad spectrum antiviral compound ribavirin. Moreover,  
14  
15  
16  
17 time of addition experiments highlighted that compounds likely act in the first phases of  
18  
19  
20  
21 WNV replication. Finally, ADME analysis of the most potent derivatives revealed 100-  
22  
23  
24 times improved aqueous solubility with respect to the hit **1**, thus allowing to overcome  
25  
26  
27  
28 an important limitation of our compound.  
29  
30  
31  
32  
33  
34  
35  
36  
37  
38  
39  
40  
41  
42  
43  
44  
45  
46  
47  
48  
49  
50  
51  
52  
53  
54  
55  
56  
57  
58  
59  
60

## RESULTS AND DISCUSSION

### Molecular modelling

With the purpose of identifying novel small molecules inhibitors of the DDX3X helicase binding site, we analyzed the docking poses of our hit compounds **1** and **2** within the DDX3X RNA binding pocket. The 3D structure of DDX3X in its RNA-bound closed conformation previously generated by homology modeling<sup>20</sup> was used to perform our studies. As shown in Figure 2A, the docking analysis of compound **2** highlighted favorable hydrogen bond interactions between the nitrobenzene oxygen atom and Arg276 and Gly325, as well as between the sulfonamide group and Pro274 and Arg480, while the hydroxyl substituent is engaged in profitable H-bond interaction with the residues Pro274 and Arg503. Furthermore, hydrophobic interactions were found with Phe357, Val500, and Arg503. The predicted binding mode of compound **1** (Figure 2A) confirmed some key interactions as seen for compound **2**, more in detail the triazole ring interacted with the guanidine group of Arg276, whereas the urea NH groups and carbonyl moiety were involved in hydrogen bonds with Pro274 and Arg480 respectively.

Moreover, the butyl terminus established beneficial interactions with Arg326 and Gly302. Finally, the tolyl ring established hydrophobic contacts with Arg503 and Pro274 side chains, and the phenyl ring made hydrophobic interactions with Phe357.

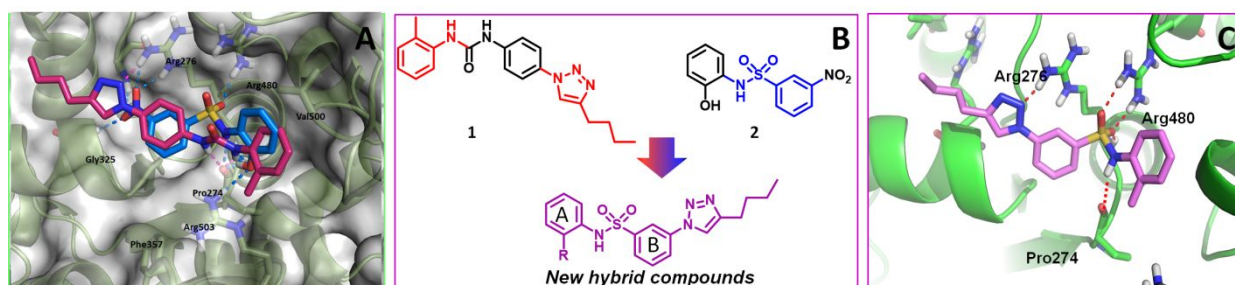
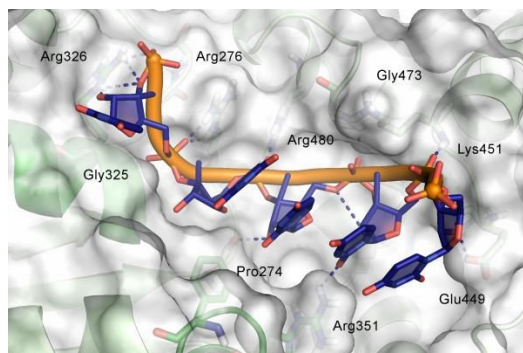


**Figure 2:** A) Overlapped binding mode of compound 1 (pink) and 2 (blue marine) in DDX3X helicase pocket. Main interactions of both compounds with key residues of the active site are highlighted. Remarkably, Arg276, Arg480 and Gly302 take important contacts also with RNA phosphate backbone while Gly325, Pro274 and Arg503 interact directly with the nucleobases. B) 2D structure representation of schematic idea behind the merged series design. C) Proposed binding mode for merged derivative 13.

It is worthy to note that two compounds were both able to interact with Arg276 and Arg480 and to take profitable contacts also with Gly325, Pro274 and Arg503 that our

1  
2  
3 computational model<sup>20</sup> suggested to be important in RNA strand interactions into the  
4  
5  
6  
7 helicase binding site (Figure 3).  
8  
9



10  
11  
12  
13  
14  
15  
16  
17  
18  
19  
20  
21  
22  
23 **Figure 3.** Surface and cartoon representation of RNA's main interactions of within the  
24  
25  
26 helicase binding site of our homology model.  
27  
28  
29

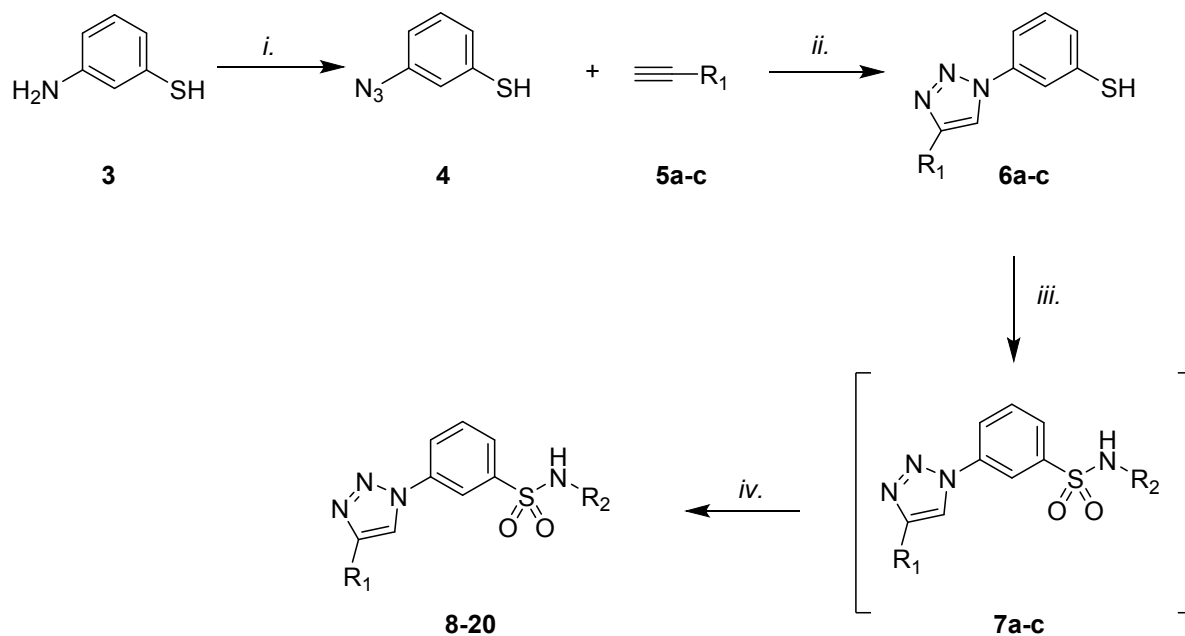
30  
31 Starting from this analysis, we merged the key structural units of **1**<sup>19</sup> and **2**<sup>20</sup> to provide a  
32  
33  
34 new series of compounds able to interact at the same time with most of the residues  
35  
36  
37 involved in the binding of both of them, with a particular attention to Arg276, Pro274 and  
38  
39  
40 Arg480 since their suggested role in RNA strand binding. To this aim, as shown in  
41  
42  
43  
44 Figure 2B, the n-alkyl substituted triazole group was selected from **1** structure, while the  
45  
46  
47 phenyl-substituted sulfonamide moiety was chosen from the structure of compound **2**;  
48  
49  
50  
51 the 'hybrid' structure was finally composed by using the common aromatic ring (B) as  
52  
53  
54  
55  
56  
57  
58  
59  
60

1  
2  
3 linker and a small library of compounds were designed around this starting structure to  
4  
5  
6  
7 explore the chemical space in relation to the activity against DDX3X.  
8  
9  
10  
11  
12  
13  
14  
15  
16  
17  
18  
19  
20  
21  
22  
23  
24  
25  
26  
27  
28  
29  
30  
31  
32  
33  
34  
35  
36  
37  
38  
39  
40  
41  
42  
43  
44  
45  
46  
47  
48  
49  
50  
51  
52  
53  
54  
55  
56  
57  
58  
59  
60

## Chemistry

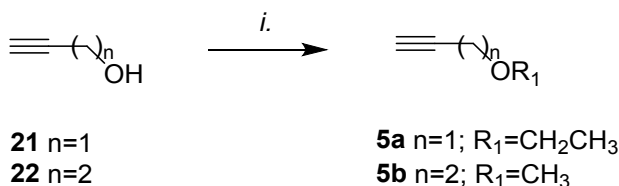
The synthesis of compounds was accomplished following the synthetic route reported in Scheme 1. Aminothiophenol **3** was first converted into azide **4** by diazotization, subsequent click reaction with the opportune terminal alkynes **5a-c** provides triazoles **6a-c**. Oxidative chlorination of thiols **6a-c** led to the corresponding sulfonyl chlorides intermediates that were immediately converted into final compounds **8-20** by nucleophilic reaction with the opportune aromatic amines.

### Scheme 1. Synthesis of sulfonamides 8-20.



1  
2  
3  
4 Reagents and conditions: *i.* a) *t*-BuONO, ACN, 20 min. 0°C; b) TMSN<sub>3</sub>, ACN, 2h r.t.; *ii.*  
5  
6  
7 CuSO<sub>4</sub>·5 H<sub>2</sub>O, sodium ascorbate, H<sub>2</sub>O *t*-BuOH (1:1), MW 10 min, 120°C; *iii.* H<sub>2</sub>O<sub>2</sub>,  
8  
9  
10 SOCl<sub>2</sub>, ACN, from 0 °C to rt, 15 min; *iv.* opportune amine, Pyridine (dry), 5h r.t.  
11  
12  
13

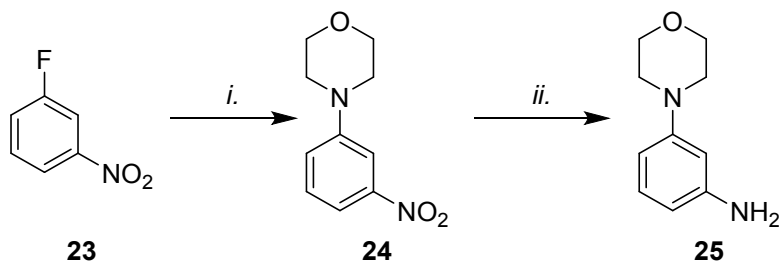
14  
15 **Scheme 2. Synthesis of ethers 5a-b.**



24 Reagents and conditions: *i.* a) NaOH (aq) (6M), 20 min., r.t; b) dimethylsulfate or  
25  
26  
27 diethylsulfate, 60 min, 50-55°C.  
28  
29  
30  
31

32 Terminal alkynes **5a** and **5b** were respectively synthesized from propargyl alcohol and  
33  
34  
35 but-3-yn-1-ol by Haworth alkylation, and purified by distillation (Scheme 2). As shown in  
36  
37  
38  
39 Scheme 3, aniline **25** was synthesized by nucleophilic displacement of 1-fluoro-3-  
40  
41  
42 nitrobenzene **23** with morpholine in presence of K<sub>2</sub>CO<sub>3</sub> and subsequent reduction Pd on  
43  
44  
45 charcoal catalysed.  
46  
47  
48

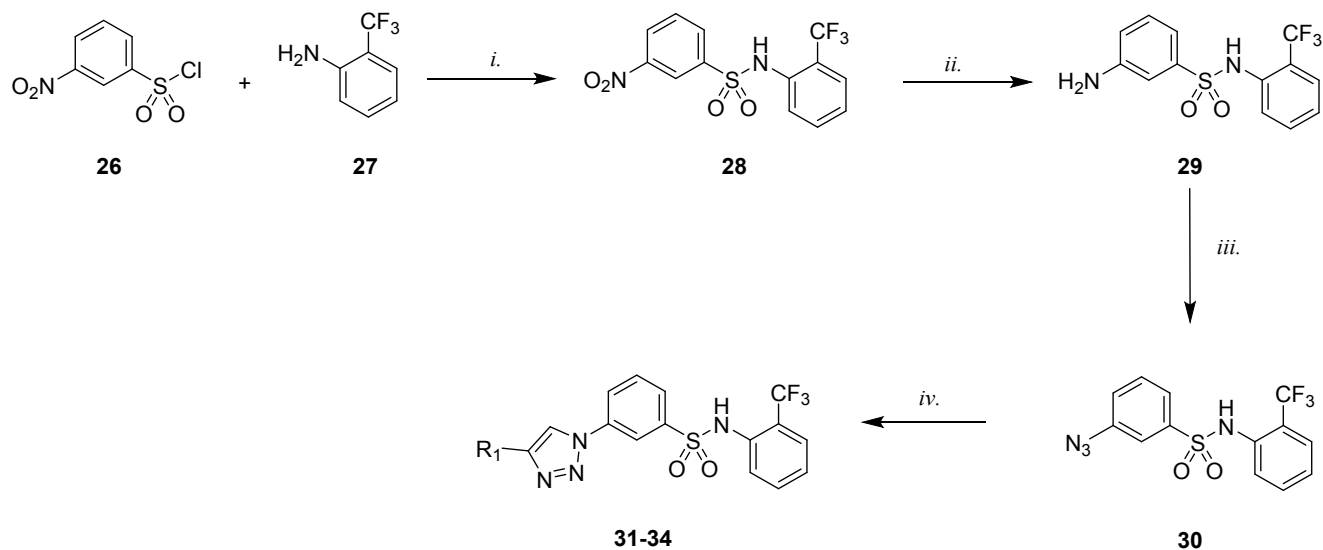
49  
50 **Scheme 3. Synthesis of aniline 25.**  
51  
52  
53  
54  
55  
56  
57  
58  
59  
60



13  
14 Reagents and conditions: *i.* a) morpholine,  $K_2CO_3$ , DMSO (dry), 3h, 200° C, *ii.*  $H_2$ , Pd/C,  
15  
16  
17 MeOH, 1h.  
18  
19

20  
21 As shown in Scheme 4, the synthetic route to the final compounds **31-34** first entailed  
22  
23 the preparation of the common azide intermediate **30**, using synthetic procedures  
24  
25 described in Scheme 1. Derivatives **31-34** were then obtained by click reaction with the  
26  
27  
28 opportune terminal alkyne. Para-substituted compounds **35** and **36** were synthesized  
29  
30  
31 analogously.  
32  
33  
34  
35  
36  
37

38  
39 **Scheme 4. Synthesis of sulfonamides 31-34.**  
40  
41  
42  
43  
44  
45  
46  
47  
48  
49  
50  
51  
52  
53  
54  
55  
56  
57  
58  
59  
60



21 Reagents and conditions: *i.* Pyr, 5h r.t. *ii.* H<sub>2</sub>, Pd/C, MeOH; *iii a)* *t*-BuONO, CH<sub>3</sub>CN, 80  
22 min. 0°C; *b)* TMSN<sub>3</sub>, CH<sub>3</sub>CN, 2h r.t.; *iv.* Opportune terminal alkyne, CuSO<sub>4</sub>·5 H<sub>2</sub>O,  
23  
24  
25  
26  
27  
28 sodium ascorbate, H<sub>2</sub>O *t*BuOH (1:1), MW 10 min, 120°C.  
29  
30  
31  
32  
33  
34  
35  
36  
37  
38  
39  
40  
41  
42  
43  
44  
45  
46  
47  
48  
49  
50  
51  
52  
53  
54  
55  
56  
57  
58  
59  
60

## Biological evaluation

Derivatives **8-20** and **31-36** were first evaluated for their ability to inhibit the helicase activity of DDX3X, results were reported in Table 1. Seven compounds showed promising inhibitory values higher than of 80% (compounds **8, 9, 10, 14, 15, 19** and **31**). The meta substitution of triazole on ring B was more favorite with respect to the para position, being **36** about 26% less active than the corresponding meta derivative **8**. This is also confirmed by the docking studies, due to the higher shape complementarity of the binding site and **8** with respect to **36**. Three dimensional conformation of the latter results to be much more constrained within the pocket, and this is likely to be responsible for the lower activity.

Replacement of triazole butyl chain with isopentyl was well tolerated (compound **31**), when the length was reduced to 2 carbons, the activity decreased of about 25% in compound **33**, in line with a lower occupancy of the binding site and poorer complementarity between ligand and protein cavity as also provided by the docking model. Yet according with this observation, the introduction of bulkier substituents such

1  
2  
3 as cyclohexyl and phenyl was detrimental for the activity which decreased to 41% and  
4  
5  
6  
7 52% for compounds **34** and **32**, respectively.  
8  
9

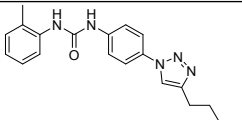
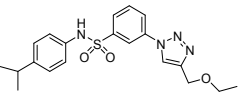
10 Alkyl chain of the triazole ring was also explored by checking the effect of introducing  
11  
12  
13 a polar atom. As a result, methyl-ethyl ether derivatives **10** and **15** retained their  
14  
15  
16  
17 activities; in contrast ethyl-methyl ether **11** was found 31% less active than the  
18  
19  
20 corresponding isomer **10**. According to our docking studies, the ether oxygen atom can  
21  
22  
23  
24 establish a hydrogen bond interaction with Arg326. In fact, in the ethyl-methyl ether  
25  
26  
27  
28 derivatives, distance between the ether oxygen atom and its counterpart is less  
29  
30  
31 favorable to the hydrogen bond interaction. On the whole, the pocket hosting the  
32  
33  
34 substituted triazole moiety requires a precise spatial disposition (meta substitution  
35  
36  
37 preferred over the para one) while preferring more flexible-less constrained triazole  
38  
39  
40  
41 substituents (butyl and isopentyl preferred over phenyl and cyclohexyl rings) occupying  
42  
43  
44  
45 as much space as possible (lower activity in the presence of ethyl substituent). Polar  
46  
47  
48 atoms are tolerated, and a proper distance to efficiently interact with Arg326 appears to  
49  
50  
51  
52 favor compound activity.  
53  
54  
55  
56  
57  
58  
59  
60

1  
2  
3 Analogously, the pocket that houses the other terminal side of our compound series,  
4  
5  
6  
7 i.e. ring A, also presents distinctive hallmarks. In particular, a proper combination of  
8  
9  
10 both polar and hydrophobic interactions appears to be beneficial to compounds' activity.  
11  
12  
13 Noteworthy, the presence of a hydrogen bond acceptor on ring A leads to high % of  
14  
15  
16 DDX3X inhibition across this chemical series, being hydrogen bond interactions feasible  
17  
18  
19  
20 with Pro274 and Arg503 of the binding pocket as revealed by our docking studies. On  
21  
22  
23 confirmation of that, the introduction of an isoquinolyl- ring (compounds **14** and **15**) on  
24  
25  
26 ring A was well tolerated as well as the -OH and the -OCH<sub>3</sub> ortho substitution  
27  
28  
29 (compounds **8** and **19**), all bearing hydrogen-bonding moieties. Also compounds **9** and  
30  
31  
32 **10**, bearing the -CF<sub>3</sub> moiety at the ortho position of ring A, satisfy such requirements,  
33  
34  
35 being the trifluoromethyl group reported to have both hydrophobic and polar (hydrogen-  
36  
37  
38 bonding) properties.<sup>23</sup> Substitution of the trifluoromethyl or hydroxyl groups of  
39  
40  
41 compounds **8**, **9**, **10** with a methyl group (compound **13**), which shows only hydrophobic  
42  
43  
44 properties, leads to a lower DDX3X % of inhibition in the sulfonamide series. Activity  
45  
46  
47 further decreases in the presence of a fluorine or hydrogen substituents (compounds **12**  
48  
49  
50 and **20**) which have similar % of inhibition values. Lower activity of compound **12** is  
51  
52  
53  
54  
55  
56  
57  
58  
59  
60

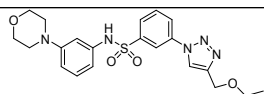
likely to be due to the lower occupancy combined with a less effective hydrogen bonding interaction, both exerted by the fluorine atom, the unsubstituted derivative **20** likewise showed a reduced activity value of 31%. The abolishment of the activity for compound **16**, where a morpholine moiety was introduced on ring A, is explained by docking studies to be due to the spatial constraints of region of the binding site, being able to accommodate the planar isoquinoline system but unfavorable to host the morpholine ring.

Also, the ortho position of the substituents on ring A results to be preferred, although the para- methoxy substitution of derivative **18** is tolerated with a slight loss of activity. Unfortunately, the low solubility of **17** and **35** limited their enzymatic evaluation.

**Table 1.** DDX3X anti-enzymatic activity.

Cmpd.ID <sup>[a]</sup>	Structure	Inhibition <sup>[b]</sup> (%)	Cmpd.ID <sup>[a]</sup>	Structure	Inhibition <sup>[b]</sup> (%)
<b>1</b>		98±1	<b>17</b>		nd

2		98±2	18		80±1
8		83±3	19		98±0.5
9		98±1	20		31±2
10		98±0.5	31		96±1
11		67±2	32		52±2
12		24±2	33		71±2
13		59±2	34		41±2.1
14		99±0.5	35		nd
15		98±1	36		57±0.5

1  
2  
3  
4  
5  
6  
7  
8  
9  
10  
11  
12  
13  
14  
15  
16  
17  
18  
19  
20  
21  
22  
23  
24  
25  
26  
27  
28  
29  
30  
31  
32  
33  
34  
35  
36  
37  
38  
39  
40  
41  
42  
43  
44  
45  
46  
47  
48  
49  
50  
51  
52  
53  
54  
55  
56  
57  
58  
59  
60  
**16**

na

[a] Data represent mean two values of the least two experiments. [b] % inhibition at a fixed concentration of 20  $\mu$ M.  
na: not active. nd: not determined, compound precipitated from medium

The docking studies suggested that compounds could act as competitive inhibitors in the helicase binding site. In order to prove our hypothesis, we generated dose-response curves titrating compound **8** in DDX3X helicase assays, in the presence of increasing fixed concentrations of the RNA substrate. As shown in the new Figure 4, the inhibitory potency (ID50) of the compound decreased (higher absolute values) as the RNA concentrations increased. This is consistent with the hypothesized competitive mechanism of inhibition, with respect to the RNA substrate.

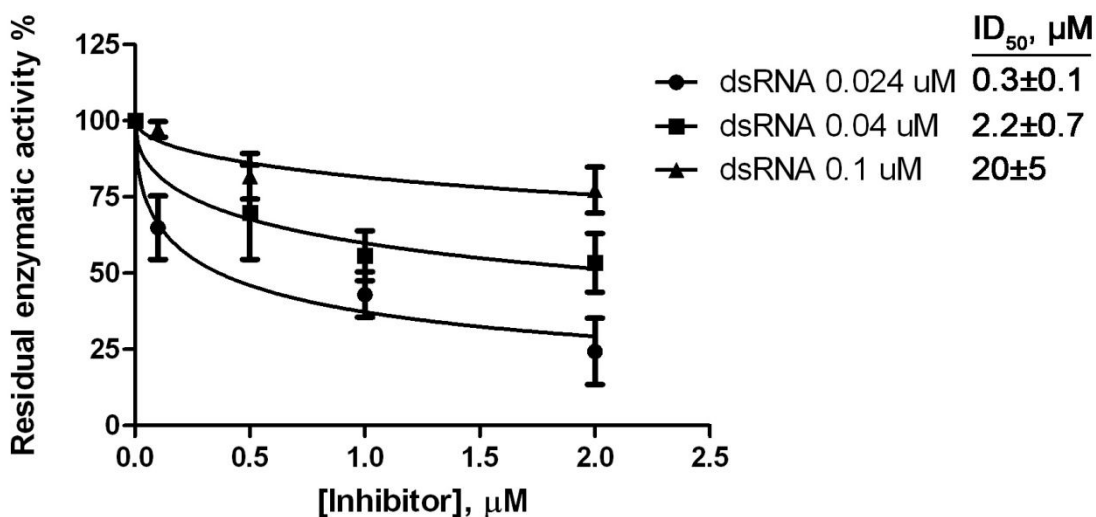


**Figure 4.** Increasing concentrations of the inhibitor **8** were titrated in helicase assays, in the presence of 30 pmols of DDX3X and increasing fixed concentrations of the dsRNA substrate. Values are the mean of three independent measurements  $\pm$  S.D. The residual enzymatic activity values were plotted as a function of the inhibitor concentrations and the corresponding ID<sub>50</sub> values calculated for each dsRNA concentration are indicated on the right side of the panel.

The compounds described here have been rationally designed to specifically target the helicase activity of DDX3X. In order to confirm the selectivity of our compounds, we tested the ability of **1**, **2**, **9** and **14** to inhibit the ATPase activity of DDX3X and the

1  
2  
3 helicase activity of the related human DEAD-box helicase DDX1. As shown in Table 2,  
4  
5  
6  
7 no inhibition was found with any compound concentration.  
8  
9

10 **Table 2.** Enzymatic data on selected compounds  
11

Cpd ID	ATPase DDX3 IC <sub>50</sub> , μM	DDX1 IC <sub>50</sub> , μM
1	>200 <sup>[a]</sup>	>200 <sup>[a]</sup>
2	>200 <sup>[a]</sup>	>200 <sup>[a]</sup>
9	>200 <sup>[a]</sup>	>200 <sup>[a]</sup>
14	>200 <sup>[a]</sup>	>200 <sup>[a]</sup>

12  
13  
14  
15  
16  
17  
18  
19  
20  
21  
22  
23 [a] The value >200 indicates that less than 20% of inhibition was observed at 200 μM,  
24 the highest concentration tested.  
25  
26  
27  
28

29 Then, we quantified the cellular concentrations of the protein DDX3X, in order to  
30  
31 confirm the presence of our target before carrying out anti-WNV and cytotoxicity assays.  
32  
33

34  
35 As reported in Table 3, African green monkey kidney epithelial (VERO) cells are  
36  
37 endowed by a DDX3X concentration of 421 nM, higher than adenocarcinomic human  
38  
39 alveolar basal epithelial cells (A549) but lower than human hepatocellular carcinoma  
40  
41 cell line Huh-7 (respectively valued 103 nM and 755 nM).  
42  
43  
44  
45  
46  
47  
48  
49

50 **Table 3.** DDX3X cellular expression in Huh-7, A549 and VERO<sup>[a]</sup>.  
51

Huh-7 <sup>[b]</sup>	VERO <sup>[c]</sup>	A549 <sup>[d]</sup>

---

<b>DDX3X (nM)</b>	755±170	421±140	103±20
-------------------	---------	---------	--------

---

[a] Values represent mean±S.D of three independent experiments. For details see Methods [b] Evaluated in Huh7: Hepato cellular carcinoma cells. [c] Evaluated in VERO: African green monkey kidney cells. [d] Evaluated in A549: adenocarcinomic human alveolar basal epithelial cells.

The three cell lines were infected with WNV at a MOI of 0.1, and the antiviral activity of compound **9** was assayed. As reported in Table 4 its activities seemed proportional to the DDX3X concentrations. Probably due to the DDX3X implications in pulmonary cancer<sup>25</sup>, **9** shown a cytotoxic activity of 21.3 μM. For these reasons, in order to avoid interferences due to anticancer related cytotoxic effects, the human Huh-7 cells characterized by a higher DDX3X concentration of 755 nM were chosen to perform our studies.

**Table 4.** Comparison of antiviral activities of **9** in different cell lines infected with WNV<sup>[a]</sup>.

Cpd. ID	Huh-7 <sup>[d]</sup>		VERO <sup>[e]</sup>		A549 <sup>[f]</sup>	
	EC <sub>50</sub> <sup>[b]</sup> (μM)	CC <sub>50</sub> <sup>[c]</sup> (μM)	EC <sub>50</sub> <sup>[b]</sup> (μM)	CC <sub>50</sub> <sup>[c]</sup> (μM)	EC <sub>50</sub> <sup>[b]</sup> (μM)	CC <sub>50</sub> <sup>[c]</sup> (μM)
<b>9</b>	23.1 ± 0.4	>200	12 ± 1.1	>200	3.4 ± 0.8	21.3 ± 1.1
ribavirin	90 ± 2.5	>200	95 ± 5.1	nt	46 ± 2.3	nt

[a] Data represent mean two values of the least two experiments. [b] EC<sub>50</sub>: half maximal effective concentration or needed concentration to inhibit 50% viral induced cell

1  
2  
3  
4 death [c]  $CC_{50}$  Cytotoxic concentration 50 or needed concentration to induce 50% death  
5 of non-infected cells [d] Evaluated in Huh7: Hepato cellular carcinoma cells. [e]  
6 Evaluated in VERO : African green monkey kidney cells. [f] Evaluated in A549:  
7 adenocarcinomic human alveolar basal epithelial cells. Ribavirin was used as a  
8 reference compound. Nt= not tested  
9  
10  
11  
12  
13  
14  
15  
16

17 Subsequently, Huh-7 cells were infected with WNV, and compounds endowed with  
18  
19 the best  $IC_{50}$ s against DDX3X were assayed for their antiviral properties. As reported in  
20  
21 Table 5, compounds showed interesting antiviral activities, ranging from 2.3 to 65.9  $\mu$ M,  
22  
23 comparable or even higher than the broad spectrum antiviral ribavirin, which was used  
24  
25 as a reference compound. Compound **8** showed the highest antiviral activity value of  
26  
27 2.3  $\mu$ M, followed by **15**, **9**, **13**, **14** and **10**. All these compounds had comparable anti-  
28  
29 enzymatic profiles; the overall trend of their cellular activities could be ascribed to their  
30  
31 different physico-chemical parameters, which may influence the cellular penetration,  
32  
33 and consequently the antiviral effects. Compound **15** resulted to be particularly  
34  
35 promising, since it showed a good antiviral activity together with favorable aqueous  
36  
37 solubility, 100 times higher than hit compound **1**. Compound **2** showed the lowest  
38  
39 activity, probably due to the limited cellular permeability (see ADME Section Table 6).  
40  
41  
42  
43  
44  
45  
46  
47  
48  
49  
50  
51  
52  
53  
54  
55  
56  
57  
58  
59  
60

The mild antiviral activity of compound **13** is in line with its % inhibition of about 60% against DDX3X and was considered not worthy of further investigation Finally, compound **12** endowed with the worst DDX3X inhibitory activity was found to be inactive in the cell-based assay.

**Table 5.** Antiviral activities and cytotoxicity of selected compounds against WNV infected Huh-7 cells<sup>[a]</sup>.

Cpd. ID	WNV <sup>[d]</sup>	Huh-7
	EC <sub>50</sub> <sup>[b]</sup> ( $\mu$ M)	CC <sub>50</sub> <sup>[c]</sup> ( $\mu$ M)
1	8.8 $\pm$ 0.2	>200
2	120 $\pm$ 5.2	175 $\pm$ 11
8	2.3 $\pm$ 0.5	>200
9	23.1 $\pm$ 0.4	>200
10	65.9 $\pm$ 2.3	>200
12	>200	>200
13	39.9 $\pm$ 1.1	>200
14	55 $\pm$ 1.1	>200
15	13 $\pm$ 0.8	>200
ribavirin	95.5 $\pm$ 3.2	>200

[a] Data represent mean  $\pm$  standard deviation of three experiments. [b] EC<sub>50</sub>: half maximal effective concentration or needed concentration to inhibit 50% viral induced cell death [c] CC<sub>50</sub> Cytotoxic concentration 50 or needed concentration to induce 50% death of non-infected cells [d] evaluated in Huh7 cells. Nt= not tested. Ribavirin was used as a reference compound.

1  
2  
3  
4  
5  
6  
7 In order to better evaluate the antiviral activities of our compounds, we selected **9** as  
8  
9  
10 representative of the series, to investigate the mechanism of action (Figure 5). Time of  
11  
12  
13 addition studies, performed at compound inhibitory concentration near and under the  
14  
15  
16  
17  $IC_{50}$  values, clearly demonstrated that **9** acted in the first two hours of WNV life cycle,  
18  
19  
20 since the addition of **9** after 3 hours post infection did not affect viral replication (Figure  
21  
22  
23  
24 5 A). In particular, although an antiviral effect was visible when added before viral  
25  
26  
27 infection, and cell-entry occurred, the substantial activity of the compound **9** also after  
28  
29  
30 two hours of infection could be indicative that its main target activity was in a  
31  
32  
33 subsequent steps of the viral replication. Consequently, we evaluated the effect of **9** in  
34  
35  
36 the production of both genomic and complementary viral RNA. Importantly, our inhibitor  
37  
38  
39 was able to interfere with the concentration of genomic RNA in the early time of  
40  
41  
42 infection (from 2 h to 12 h post infection) only when added 1 h post infection without  
43  
44  
45 significant changes when added 3 h post infection. Moreover, although the  
46  
47  
48  
49 complementary RNA was not revealed up to 12 hours post infection, 24 h post infection  
50  
51  
52 the quantity of complementary RNA was slit lower after the addition of compound **9** 1 h  
53  
54  
55  
56  
57  
58  
59  
60

1  
2  
3  
4 post infection. Moreover our inhibitor was able to interfere marginally with the  
5  
6  
7 concentration of genomic RNA, without significant changes in the quantity of the  
8  
9  
10 complementary not infective RNA. Finally, we evaluated its effect on the production of  
11  
12  
13 WNV nucleocapsid protein (NC). As highlighted in Figure 5 C, the addition of **9** 1h post  
14  
15  
16 infection significantly reduced the concentration of NC, while, according to the results  
17  
18  
19 shown in panel C, its addition after 3 hours did not change NC concentrations, which  
20  
21  
22 were comparable to the control. Overall, these results suggested a possible implication  
23  
24  
25 of **9** in the first phases of viral replication, probably during protein translation, after the  
26  
27  
28 entry process.  
29  
30  
31  
32  
33  
34  
35  
36  
37  
38  
39  
40  
41  
42  
43  
44  
45  
46  
47  
48  
49  
50  
51  
52  
53  
54  
55  
56  
57  
58  
59  
60

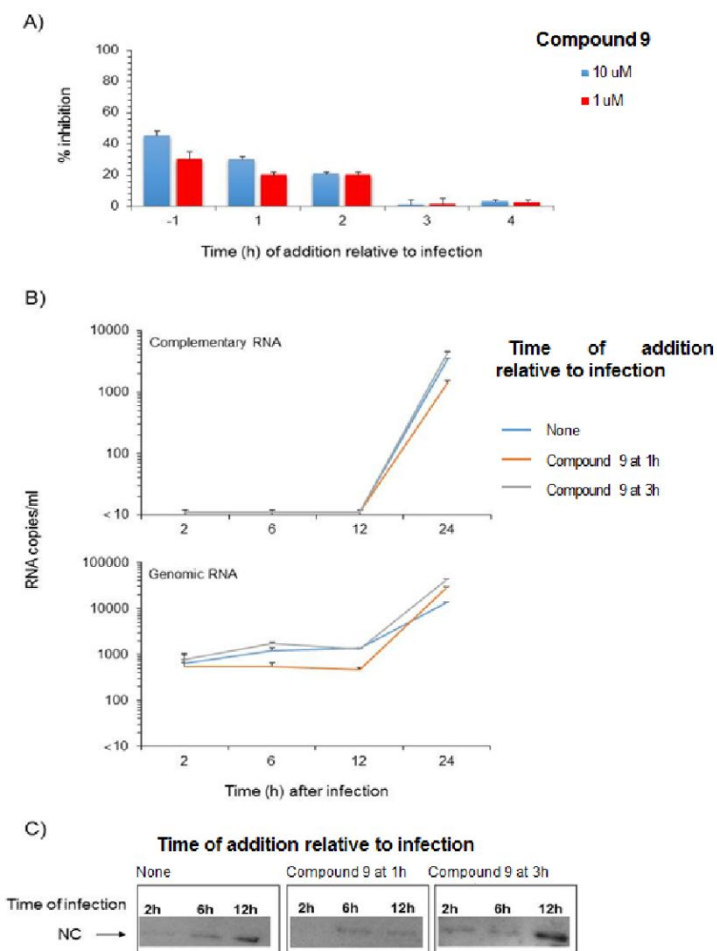


**Figure 5:** Effect of varying anti-DDX3X compound 9 time of administration on WNV replication. A) WNV infection of Huh7 cells at MOI of 0.1 in presence of compound 9 at 1 $\mu$ M and 10  $\mu$ M added at indicated time (h) relative to the infection and assayed with the viral plaque reduction assay. Data represent means  $\pm$  standard deviation. B) WNV genomic and complementary viral RNA in Huh7 cells assayed after infection in absence or in presence of compound 9 at 1  $\mu$ M added at 1 h and 3 h of the infection. Data

1  
2  
3 represent means  $\pm$  standard deviation. C) WNV capsid protein electrophoretic mobility  
4  
5  
6  
7 obtained from Huh7 cells after infection in absence or in presence of compound **9** at 1  
8  
9  
10  $\mu$ M added at 1 h and 3 h of the infection. None, no compound **9** addition.  
11  
12  
13  
14  
15  
16  
17  
18  
19  
20  
21  
22  
23  
24  
25  
26  
27  
28  
29  
30  
31  
32  
33  
34  
35  
36  
37  
38  
39  
40  
41  
42  
43  
44  
45  
46  
47  
48  
49  
50  
51  
52  
53  
54  
55  
56  
57  
58  
59  
60

### In vitro ADME analysis

Compounds **2**, **8**, **9**, **10**, **14** and **15** were *in vitro* profiled for aqueous solubility, liver microsomal stability and membrane permeability. As reported in table 6 compounds were characterized by improved aqueous solubility values, in particular compounds **14**, **15** and **10**, even if less active against WNV than compound **1** are about 100-times more soluble than hit compound **1** with LogS comparable to that of **2**. Furthermore, passive membrane permeability assay (PAMPA) indicated not limiting values with the exception of hit compound **2**, that showed a value minor of  $0.1 \cdot 10^{-6}$  cm/sec that is probably the cause of its inactivity in antiviral assay. Finally, stability tests in human liver microsomes (HLM) disclosed that all the selected compounds showed a high metabolic stability major of 95.6%.

**Table 6.** *In vitro* ADME analysis of selected compounds

Cpd. ID	AppP <sup>[a]</sup>	LogS <sup>[b]</sup>	HLM Stability <sup>[c]</sup>
<b>1</b>	$2.86 \cdot 10^{-6}$	-7.05	99.0±0.6
<b>2</b>	$<0.1 \cdot 10^{-6}$	-4.36	98.3±1.1
<b>8</b>	$0.1 \cdot 10^{-6}$	-7.5	95.6±0.8

<b>9</b>	$0.21 \cdot 10^{-6}$	-7.5	99.0±1.2
<b>10</b>	$0.71 \cdot 10^{-6}$	-4.6	97.1±0.6
<b>14</b>	$0.68 \cdot 10^{-6}$	-5.4	98.0±0.9
<b>15</b>	$0.44 \cdot 10^{-6}$	-4.7	96.0±0.4

[a] Apparent permeability reported in  $\text{cm} \cdot \text{s}^{-1}$ . [b] Aqueous solubility expressed as Log of molar concentration. [c] Human Liver Microsomal Metabolic Stability

## Conclusions

We identified a completely new family of selective inhibitors of the helicase activity of DDX3X. The compounds described here have been rationally designed to specifically target the helicase activity of DDX3X. Accordingly, they were inactive in the ATPase assay and in the helicase assay against the related human DEAD-box helicase DDX1. Future plans for improving the assessment of selectivity of our compounds include their evaluation on a broader panel of DDX-family helicases, as well as the exploitation of Huh-7 cells with inducible silencing of DDX3X expression. Both approaches are currently under development in our laboratory and will be the subject of future communications. Among the 21 compounds reported, six of them (namely compounds **8**, **9**, **10**, **13**, **14** and **15**) are characterized by promising antiviral activities against WNV, lower than the broad spectrum antiviral ribavirin, and more importantly without signs of cellular toxicities. It is worth to point out that the antiviral activities are DDX3X-dependant, since compound **12**, endowed with the worst inhibitory activity, did not show any antiviral effect up to 200  $\mu$ M. Furthermore, merged derivatives **10**, **14** and **15**, even if less active against WNV than compound **1**, are endowed with a very good aqueous

1  
2  
3 solubility, with values 100-times higher than the hit 1, thus overcoming an important  
4  
5  
6  
7 limitation of the previously published compounds. Furthermore, time of addiction  
8  
9  
10 experiments are consistent with literature studies previously published on DDX3X  
11  
12  
13 recruitment on WNV replication site<sup>22</sup> highlighting an involvement of our compounds in  
14  
15  
16 the first phases of WNV replication and suggesting their possible role in the step of  
17  
18  
19 protein translation, after the entry process. Noteworthy, although tolerability and  
20  
21  
22 bioavailability need to be proved in vivo, the effectiveness of the compounds also when  
23  
24  
25 added before viral cell-infection suggest their possible use as prophylactic antiviral  
26  
27  
28 drugs. Even if we are aware that deep investigations are needed to elucidate the  
29  
30  
31 mechanism of action of our compounds, to date the exact implications of our own target  
32  
33  
34 on the WNV life cycle remain poorly understood.  
35  
36  
37  
38  
39  
40

41  
42 In the absence of any available antiviral compound for the treatment of WNV  
43  
44  
45 infection<sup>24</sup> the present study confirms our previous findings, suggesting that DDX3X  
46  
47  
48 helicase inhibitors can represent the Achilles' hell of viruses and that human proteins  
49  
50  
51 can be manipulated to fight novel emerging viral threats.  
52  
53  
54  
55  
56  
57  
58  
59  
60

## METHODS

### Docking studies

All compounds studied herein were docked within the RNA binding site of the modeled human DDX3X closed conformation previously published<sup>20</sup> using the software package GOLD 4.1<sup>26,27</sup>. The pocket under investigation was inserted into a grid box centred on residue Phe357 and enclosing residues lying within 10 Å from such amino acid. The genetic algorithm parameter settings were employed using the search efficiency set at 100%, and 100 runs were carried out for each ligand. Chemscore was chosen as the fitness function. Finally, results differing less than 1.5 Å in ligand-all atom RMSD were clustered together. For each inhibitor, the first ranked solution was selected for further analysis. Pictures of the modeled ligand-enzyme complexes together with graphic manipulations were rendered using the PyMOL molecular graphic system.<sup>28</sup>

### Chemistry

Reagents were obtained from commercial suppliers (for example Sigma-Aldrich, Alfa Aesar). All commercially available chemicals were used as purchased without further purification. CH<sub>2</sub>Cl<sub>2</sub> and MeOH were dried prior to use by distilling from calcium hydride or magnesium methoxide. Anhydrous reactions were run under a positive pressure of dry N<sub>2</sub> or argon. TLC was carried out using Merck TLC plates silica gel 60 F254. Chromatographic purifications were performed on columns packed with Merck 60 silica gel, 23-400 mesh, for flash technique.

All NMR spectra were recorded on Bruker Avance DPX400 spectrometer at 400 MHz for <sup>1</sup>H-NMR or 100 MHz for <sup>13</sup>C-NMR. Chemical shifts are reported relative to tetramethylsilane at 0.00 ppm. <sup>1</sup>H patterns are described using the following abbreviations: s = singlet, d = doublet, t

1  
2  
3 = triplet, q = quartet, quint = quintet, sx = sextet, sept= septet, m = multiplet, br = broad signal,  
4  
5 br s = broad singlet.  
6

7  
8 Mass spectra (MS) data were obtained using an Agilent 1100 LC/MSD VL system (G1946C)  
9  
10 with a 0.4 mL/min flow rate using a binary solvent system 25 of 95:5 methyl alcohol/ water. UV  
11  
12 detection was monitored at 254 nm. Mass spectra were acquired in positive and negative mode  
13  
14 scanning over the mass range.  
15

16  
17 **Microwave irradiation experiments** were conducted using CEM Discover Synthesis Unit  
18  
19 (CEM Corp., Matthews, NC). The machine consists of a continuous focused microwave power  
20  
21 delivery system with operator selectable power output from 0 to 300W. The temperature of the  
22  
23 contents vessels was monitored using calibrate infrared temperature control mounted under the  
24  
25 reaction vessel. All the experiments were performed using a stirring option whereby the contents  
26  
27 of the vessels are stirred by means of rotating magnetic plate located below the floor of the  
28  
29 microwave cavity and a Teflon- coated magnetic stir bar in the vessel.  
30  
31

32  
33 **UV/LC-MS method** For the quantitative analysis was used an UV/LC-MS system. LC analysis  
34  
35 were performed by Agilent 1100 LC/MSD VL system (G1946C) (Agilent Technologies, Palo  
36  
37 Alto, CA) constituted by a vacuum solvent degassing unit, a binary high-pressure gradient pump,  
38  
39 an 1100 series UV detector and a 1100 MSD model VL benchtop mass spectrometer was used.  
40  
41 The Agilent 1100 series mass spectra detection (MSD) single-quadrupole instrument was  
42  
43 equipped with the orthogonal spray API-ES (Agilent Technologies, Palo Alto, CA). Nitrogen  
44  
45 was used as nebulizing and drying gas. The pressure of the nebulizing gas, the flow of the drying  
46  
47 gas, the capillary voltage, the fragmentor voltage and the vaporization temperature were set at 40  
48  
49 psi, 9 L min<sup>-1</sup>, 3000 V, 70 V and 350°C, respectively. UV detection was monitored at 280 nm.  
50  
51 The LC-ESI-MS determination was performed by operating the MSD in the positive ion mode.  
52  
53  
54  
55  
56  
57  
58  
59  
60

1  
2  
3 Spectra were acquired over the scan range  $m/z$  50-1500 using a step size of 0.1 u.  
4  
5 Chromatographic analysis was performed using a Varian Polaris 5 C18-A column (150 x 4.6  
6  
7 mm, 5  $\mu$ m particle size) at room temperature. Analysis was carried out using gradient elution of  
8  
9 a binary solution; eluent A was ACN, while eluent B consisting of water. The analysis started at  
10  
11 0% A for three minutes, then rapidly increased up to 98% in 12 min and finally remaining at  
12  
13 98% A until 18 min. The analysis was performed at flow rate of 0.8 mL min<sup>-1</sup> and injection  
14  
15 volume was 20  $\mu$ L. LC retention times, molecular ion ( $m/z$ ) and LC purity (by UV) were based  
16  
17 on the method below. Purity of compounds (as measured by peak area ratio) was >97%.  
18  
19

20  
21  
22 **3-azidobenzenethiol (4):** 3-aminothiols (2.0g, 15.97mmol) was dissolved in CH<sub>3</sub>CN and cooled  
23  
24 to 0°C in an ice-salt bath. To this stirred solution, was added tBuONO (2.84 mL, 23.9mmol), and  
25  
26 the mixture was stirred for 10 min, after this time, TMSN<sub>3</sub> (2.53 mL, 19.17mmol) was added  
27  
28 dropwise, during 10 minutes, and the resulting brown solution was stirred at r.t. One hour later  
29  
30 the solvent was removed at reduced pressure and the residue was purified by flash  
31  
32 chromatography on silica gel. Purification Eluent: EP/EA 8:2, Yield 80%. Pale white solid. <sup>1</sup>H  
33  
34 NMR: (400 MHz, CDCl<sub>3</sub>)  $\delta$  7.3-7.2 (m, 2H), 7.1 (s, 1H) 6.9 (d,  $J=6.4$  Hz, 1H)ppm.  
35  
36  
37  
38  
39

40  
41 *General procedure for the preparation of compounds 5a and 5b.*

42  
43 To a stirring solution of 200 g of NaOH in 300 mL of water (0.3 mol, 16.8 g) was added the  
44  
45 opportune alcohol (2.5 mL, 33.02 mmol). To this, was slowly added the corresponding sulfate  
46  
47 (15mmol, 2082 mg) in 2 h dropwise and the mixture was heated at 50°C. The final product was  
48  
49 distilled off, the distillation was stopped at 95 °C, then the content of the receiver was washed  
50  
51 with cold NH<sub>4</sub>Cl aq solution and separated.  
52  
53  
54  
55  
56  
57  
58  
59  
60

1  
2  
3 **3-ethoxyprop-1-yne (5a).** Yield 68% colourless oil. <sup>1</sup>H NMR (400 MHz, CDCl<sub>3</sub>-d): δ 4.13-4.13  
4 (d, *J*= 2.4 Hz, 2H), 3.60-3.55 (q, *J*=6.9 Hz 2H), 2.41-2.40 (t, *J*= 4.8 Hz, 1H), 1.24-1.22 (t, *J*=6.9  
5 Hz, 3H) ppm  
6  
7  
8  
9

10  
11 **4-methoxybut-1-yne (5b).** Yield 52% colourless oil. <sup>1</sup>H NMR (400 MHz, CDCl<sub>3</sub>-d): δ 3.52-3.49  
12 (m, 2H), 3.33 (s, 3H), 2.47-2.43 (m, 2H), 1.99-1.97 (m, 1H) ppm.  
13  
14  
15

16  
17 *General procedure for the preparation of triazoles (6a-c).* The appropriate alkyne (6.08 mmol)  
18 and the opportune azide (5.07 mmol) were suspended in a 1:1 mixture of water and *t*-BuOH (1.5  
19 mL each) in a 10 mL glass vial equipped with a small magnetic stirring bar. To this, was added  
20 sodium ascorbate (2.5 mmol) and copper(II) sulfate pentahydrate (2.50 mmol). The mixture was  
21 then heated for 10 min. at 80°C under microwave irradiation, using an irradiation power of  
22 300W. After that time the solvent was removed at reduced pressure water was added and the  
23 mixture was extracted with EtOAc (3x 20 mL). The organic layers were collected, washed with  
24 Brine and dried over Na<sub>2</sub>SO<sub>4</sub>. The crude was purified by flash chromatography on silica gel  
25 using the opportune eluent to give the desired triazole compounds.  
26  
27  
28  
29  
30  
31  
32  
33  
34  
35  
36  
37

38 **3-(4-(ethoxymethyl)-1H-1,2,3-triazol-1-yl)benzenethiol (6a):** Purification Eluent EP/EA 7:3,  
39 white solid Yield: 62%, <sup>1</sup>H NMR:(400 MHz, MeOD) δ 7.97 (s, 1H), 7.94 (s, 1H), 7.60-7.57 (m,  
40 2H), 7.49 (t, *J*=8.0 Hz, 1H), 4.70 (s, 2H), 3.66 (q, *J*=6.8 Hz, 2H), 0.89 (t, *J*=6.8 Hz, 3H) ppm.  
41  
42  
43  
44  
45

46 **3-(4-(2-methoxyethyl)-1H-1,2,3-triazol-1-yl)benzenethiol (6b):** Purification Eluent EP/EA 7:3,  
47 white solid Yield: 50%, <sup>1</sup>H NMR (400 MHz, MeOD) δ 8.02 (s, 1H), 7.45 – 7.29 (m, 2H),  
48  
49  
50  
51  
52  
53  
54  
55  
56  
57  
58  
59  
60

1  
2  
3 7.28 (d,  $J = 7.4$  Hz, 1H), 7.18 (t,  $J = 7.5$ , 1H), 3.75 (t,  $J = 6.6$  Hz, 2H), 3.38 (s, 3H), 2.97  
4  
5  
6  
7 (t,  $J = 6.6$  Hz, 2H).  
8  
9

10  
11 **3-(4-butyl-1H-1,2,3-triazol-1-yl)benzenethiol (6c)**: Purification Eluent EP/EA 8:2. Pale white  
12 solid, Yield: 78%.  $^1\text{H}$  NMR: (400 MHz,  $\text{CDCl}_3$ )  $\delta$  7.95 (s, 1H), 7.72 (s, 1H), 7.6-7.53 (m, 2H),  
13  
14 7.47 (t,  $J=8.0$  Hz, 1H), 2.81 (t,  $J=7.6$  Hz, 2H), 1.75-1.67 (m, 2H), 1.47-1.39 (m, 2H), 0.97 (t,  
15  
16  $J=7.6$  Hz, 3H) ppm.  
17  
18  
19  
20

### 21 **General procedure for the synthesis of sulfonamides 8-20.**

22  
23

24 The opportune benzenethiol (6a-c) (0.43 mmol) was dissolved in 2mL of acetonitrile, to this 30%  
25  $\text{H}_2\text{O}_2$  (1.2 mmol, 133 $\mu\text{L}$ ) and  $\text{SOCl}_2$  (0.43 mmol, 31  $\mu\text{L}$ ) were added, and the corresponding  
26  
27 solution was stirred at room temperature for 30 minutes. After this time the reaction mixture was  
28  
29 extracted with EtOAc (3x25mL), washed with brine and dried over  $\text{Na}_2\text{SO}_4$ . The solvent was  
30  
31 removed at reduced pressure, and the resulting residue was dissolved in 5 mL of DCM. To this a  
32  
33 solution of the opportune aromatic amine in 1mL of pyridine was added drop by drop. The  
34  
35 resulting mixture was stirred at rt for 4 h. After this time water was added, and the mixture was  
36  
37 extracted with DCM (6x30mL), washed with brine and dried over anhydrous  $\text{Na}_2\text{SO}_4$ . The  
38  
39 corresponding residue was purified on silica with the opportune eluent.  
40  
41  
42  
43  
44

45  
46 **3-(4-butyl-1H-1,2,3-triazol-1-yl)-N-(2-hydroxyphenyl)benzenesulfonamide (8)**. (Purification  
47 eluent: Hexane-AcOEt 3:1). Yield 80%.  $^1\text{H}$  NMR (400 MHz, Acetone):  $\delta$  8.79-8.35 (m, 2H),  
48  
49 8.34-8.31 (m, 2H), 8.11-8.09 (d,  $J=8.0$  Hz, 1H), 7.81-7.79 (d,  $J=8.0$  Hz, 1H), 7.71-7.67 (t,  $J=8.0$   
50  
51 Hz, 1H), 7.37-7.35 (d,  $J=8.0$  Hz, 1H), 6.99-6.95, (t,  $J=8.0$  Hz, 1H), 6.81-6.77 (m, 2H), 2.84 (t,  
52  
53  $J=7.6$  Hz, 2H), 1.77-1.69 (m, 2H), 1.46-1.38 (m, 2H), 0.99 (t,  $J=7.6$  Hz, 3H);  $^{13}\text{C}$  NMR (100  
54  
55  
56  
57  
58  
59  
60

MHz, Acetone):  $\delta$  149.88, 142.46, 131.77, 137.68, 130.44, 126.66, 126.50, 124.40, 124.19, 123.58, 119.90, 119.47, 118.32, 115.59, 31.30, 24.94, 21.95, 13.19. HRMS (ESI)  $m/z$  calcd for  $C_{18}H_{19}N_4O_3S$  [M-H]<sup>-</sup> 371.1178 found 371.1180.

**3-(4-butyl-1H-1,2,3-triazol-1-yl)-N-(2-(trifluoromethyl)phenyl)benzenesulfonamide (9)**

(Purification eluent: Hexane-AcOEt 3:1). Yield 90%. <sup>1</sup>H NMR (Acetone):  $\delta$  8.78 (s, 1H), 8.41-8.37 (m, 2H), 8.18-8.16 (d,  $J=8.2$  Hz, 1H), 7.89-7.87 (d,  $J=7.6$  Hz, 1H), 7.82-7.78 (t,  $J=7.8$  Hz, 1H), 7.69-7.61 (m 2H), 7.54-7.52 (d,  $J=8$ Hz, 1H), 7.45-7.44 (t,  $J=7.4$  Hz, 1H), 2.77-2.73 (t,  $J=7.4$  Hz, 2H), 1.71-1.67 (m, 2H), 1.45-1.35 (m, 2H), 0.94-0.89 (t,  $J=8.0$  Hz, 3H) ppm. <sup>13</sup>C NMR (Acetone): 149.1, 142.66, 137.89, 134.15, 133.28, 130.93(2C), 127.40 (q,  $J_{(C-F)}=5$ Hz), 126.90, 126.28, 124.80, 123.85, 122.29 (q,  $J_{(C-F)}=273$ Hz), 119.54, 118.03, 31.22, 24.95, 21.95, 13.18ppm. HRMS (ESI)  $m/z$  calcd for  $C_{19}H_{18}F_3N_4O_2S$  [M-H]<sup>-</sup> 423.1103 found 423.1107.

**3-(4-(ethoxymethyl)-1H-1,2,3-triazol-1-yl)-N-(2-(trifluoromethyl)phenyl)**

**benzenesulfonamide (10):** (Purification eluent: PE/EtOAc 7:2) Yield 85% white solid <sup>1</sup>H NMR (400 MHz,  $CDCl_3-d$ ):  $\delta$  8.09 (1H, s), 7.99-7.97 (m, 2H), 7.79-7.75 (m, 2H), 7.60-7.47 (m, 3H), 7.26-7.22 (t,  $J=7.2$  Hz, 1H), 7.14 (s, 1H), 4.66 (s, 2H), 3.63-3.58 (q,  $J=6.8$  Hz, 2H), 1.24-1.20 (t,  $J=6.8$  Hz, 3H) ppm. <sup>13</sup>C NMR (100 MHz,  $CDCl_3-d$ ): 146.95, 144.13, 140.78, 137.44, 133.39, 130.80, 126.99, 126.07(2C), 125.84, 124.87, 124.69, 122.09, 120.58 (q,  $J_{(C-F)}=280$ Hz), 118.71, 66.39, 63.99, 15.07 ppm. HRMS (ESI)  $m/z$  calcd for  $C_{18}H_{16}F_3N_4O_3S$  [M-H]<sup>-</sup> 425.0895 found 425.0890.

**3-(4-(2-methoxyethyl)-1H-1,2,3-triazol-1-yl)-N-(2-(trifluoromethyl)phenyl)**

**benzenesulfonamide (11):** (Purification eluent: PE/EtOAc 7:2) Yield 63% white solid <sup>1</sup>H NMR (400 MHz,  $CDCl_3-d$ ):  $\delta$  8.07 (1H, s), 8.02-8.00 (d,  $J=8.0$  Hz, 1H), 7.86-7.84 (d,  $J=7.9$  Hz, 2H),

1  
2  
3 7.77-7.75 (d,  $J=7.6$  Hz, 1H), 7.61-7.50 (m, 3H), 7.28-7.24 (m, 2H), 3.72 (m, 2H), 3.394 (s, 3H),  
4  
5 3.08-3.07 (m, 2H) ppm.  $^{13}\text{C}$  NMR ( $\text{CDCl}_3$ ):  $\delta$  145.32, 139.71, 133.11, 132.91, 132.43, 129.12,  
6  
7 128.81, 127.36, 126.04 (2C), 124.09, 119.21(q,  $J(\text{C-F})=268\text{Hz}$ ), 119.1, 116.66, 115.51, 77.81,  
8  
9 59.44, 30.91 ppm. HRMS (ESI)  $m/z$  calcd for  $\text{C}_{18}\text{H}_{16}\text{F}_3\text{N}_4\text{O}_3\text{S}$   $[\text{M-H}]^-$  425.0895 found 425.0893.

10  
11  
12  
13 **3-(4-butyl-1H-1,2,3-triazol-1-yl)-N-(2-fluorophenyl)benzenesulfonamide (12):** (Purification  
14  
15 eluent: PE/EtOAc 7:2) Yield 71% white solid  $^1\text{H}$  NMR (400 MHz,  $\text{CDCl}_3$ - $d$ ): 8.07 (s, 1H), 8.02-  
16  
17 8.01 (d,  $J=8.0$  Hz, 1H), 7.77-7.76 (d,  $J=8.0$  Hz, 1H), 7.68 (s, 1H), 7.62-7.57 (m, 2H), 7.15-7.09  
18  
19 (m, 2H), 6.99-6.94 (m, 2H), 2.80-2.77 (t,  $J=7.6$  Hz, 2H), 1.74-1.66 (m, 2H), 1.46-1.37 (m, 2H),  
20  
21 0.97-0.93 (t,  $J=7.6$  Hz, 3H) ppm.  $^{13}\text{C}$  NMR (100 MHz,  $\text{CDCl}_3$ ): 157.9(d,  $J(\text{C-F})=238\text{Hz}$ ),  
22  
23 149.77, 140.75, 137.65, 130.69, 127.13, 126.59, 124.96, 124.70, 124.59, 124.38, 118.44(d,  $J(\text{C-}$   
24  
25 F)=20Hz), 115.79, 115.58(d,  $J(\text{C-F})=9\text{Hz}$ ), 31.32, 25.23, 22.26, 13.78 ppm. HRMS (ESI)  $m/z$   
26  
27 calcd for  $\text{C}_{18}\text{H}_{18}\text{FN}_4\text{O}_2\text{S}$   $[\text{M-H}]^-$  373.1134 found 373.1129.

28  
29  
30  
31  
32  
33 **3-(4-butyl-1H-1,2,3-triazol-1-yl)-N-(o-tolyl)benzenesulfonamide (13).** (Purification eluent:  
34  
35 Hexane-AcOEt 3:1). Yield 90%.  $^1\text{H}$  NMR (400MHz, Acetone):  $\delta$  8.56 (s, 1H), 8.35-8.33 (d,  
36  
37  $J=8.0$  Hz, 1H), 8.25-8.23 (d,  $J=8.0$  Hz, 1H), 8.14-8.11 (t,  $J=7.2$  Hz, 1H), 7.74-7.72 (m, 2H),  
38  
39 7.17-7.10 (m 4H), 2.77-2.73 (t,  $J=7.4$  Hz, 2H), 2.72 (s, 3H), 1.73-1.65 (m, 2H), 1.43-1.37 (m,  
40  
41 2H), 0.95-0.91 (t,  $J=7.8$  Hz, 3H) ppm.  $^{13}\text{C}$  NMR (100 MHz, Acetone): 149.06, 142.56, 137.76,  
42  
43 134.78, 134.16, 130.91, 130.72, 126.78, 126.51, 126.37, 126.28, 123.51, 119.46, 118.11 31.22,  
44  
45 24.95, 21.95, 17.18, 13.18 ppm. HRMS (ESI)  $m/z$  calcd for  $\text{C}_{19}\text{H}_{21}\text{N}_4\text{O}_2\text{S}$   $[\text{M-H}]^-$  369.1385  
46  
47 found 369.1387.

48  
49  
50  
51  
52 **3-(4-butyl-1H-1,2,3-triazol-1-yl)-N-(isoquinolin-6-yl)benzenesulfonamide (14).** (Purification  
53  
54 eluent: Hexane-AcOEt 3:1). Yield 77%.  $^1\text{H}$  NMR (400 MHz,  $\text{CDCl}_3$ - $d$ ):  $\delta$  9.23 (s, 1H), 8.42 (s,  
55  
56  
57  
58  
59  
60

1  
2  
3 1H), 8.26 (s, 1H), 7.89-7.83 (m, 4H), 7.66-7.62 (m, 3H), 7.55-7.46 (m, 2H), 2.74-2.71 (t,  $J=7.8$   
4 Hz, 2H), 1.66-1.59 (m, 2H), 1.39-1.25 (m, 2H), 0.90-0.86 (t,  $J=8.0$  Hz, 3H) ppm.  $^{13}\text{C}$  NMR (100  
5 MHz,  $\text{CDCl}_3$ -*d*): 152.43, 149.84, 142.93, 141.34, 137.68, 132.70, 131.10, 130.51, 129.38,  
6 129.01, 128.51, 127.62, 127.38, 126.85, 124.13, 118.81, 115.75, 31.36, 25.25, 22.26, 13.62 ppm.  
7  
8 HRMS (ESI)  $m/z$  calcd for  $\text{C}_{21}\text{H}_{22}\text{N}_5\text{O}_2\text{S}$   $[\text{M}+\text{H}]^+$  408.1494 found 408.1489.  
9  
10  
11  
12  
13

14  
15  
16 **3-(4-(ethoxymethyl)-1H-1,2,3-triazol-1-yl)-N-(isoquinolin-5-yl)benzenesulfonamide (15):**

17  
18  
19 Purification eluent ( $\text{CHCl}_3$ /acetone 98:2). White solid, Yield: 73%  $^1\text{H}$  NMR:  $^1\text{H}$  NMR: (400  
20 MHz,  $\text{CD}_3\text{OD}$ )  $\delta$  9.50 (s, 1H), 8.51 (s, 1H), 8.45-8.43 (m, 2H), 8.23-8.18 (m, 3H), 8.07-8.05 (d,  
21  $J=8.0$  Hz, 1H), 7.80-7.66 (m, 4H), 4.63 (s, 2H), 3.61-3.56 (q,  $J=7.2$  Hz, 2H), 1.32 (t,  $J=7.2$ , 3H)  
22 ppm  $^{13}\text{C}$  NMR (100 MHz,  $\text{CDCl}_3$ -*d*)  $\delta$  192.82, 174.69, 149.87, 146.32, 141.42, 137.79, 136.51,  
23 134.59, 132.21, 131.44, 130.80, 129.22, 126.87, 124.19, 123.06, 121.88, 118.89, 65.82, 62.91,  
24 14.31 ppm HRMS (ESI)  $m/z$  calcd for  $\text{C}_{20}\text{H}_{20}\text{N}_5\text{O}_3\text{S}$   $[\text{M}+\text{H}]^+$  410.1287 found 410.1282.  
25  
26  
27  
28  
29  
30  
31

32  
33  
34 **3-(4-(ethoxymethyl)-1H-1,2,3-triazol-1-yl)-N-(3-morpholinophenyl)benzenesulfonamide**

35  
36 **(16):** Purification eluent ( $\text{CHCl}_3$ /acetone 98:2). White solid, Yield: 64%  $^1\text{H}$  NMR: (400 MHz,  
37  $\text{CDCl}_3$ )  $\delta$  8.17 (s, 1H), 7.99 (s, 1H), 7.92 (d,  $J=7.4$  Hz, 1H), 7.79 (d,  $J=7.6$  Hz, 1H), 7.72 (s, 1H),  
38 7.59 (t,  $J=8.0$  Hz, 1H), 7.12 (t,  $J=8.4$  Hz, 1H), 6.78 (s, 1H), 6.68 (d,  $J=8.4$  Hz, 1H), 6.61 (d,  
39  $J=7.6$  Hz, 1H), 4.71 (s, 2H), 3.81 (t,  $J=4.4$  Hz, 4H), 3.64 (q,  $J=6.8$  Hz, 2H), 3.1 (t,  $J=4.4$  Hz,  
40 4H), 1.27 (t,  $J=6.8$  Hz, 3H) ppm.  $^{13}\text{C}$  NMR (100 MHz,  $\text{CDCl}_3$ -*d*)  $\delta$  152.8, 147.23, 141.24,  
41 137.34, 137.13, 130.56, 129.88, 127.23, 124.35, 120.75, 119.00, 113.20, 112.88, 109.30, 66.56,  
42 63.92(2C), 48.91 (2C), 29.70, 15.15 ppm. HRMS (ESI)  $m/z$  calcd for  $\text{C}_{21}\text{H}_{26}\text{N}_5\text{O}_4\text{S}$   $[\text{M}+\text{H}]^+$   
43 444.1706 found 444.1701.  
44  
45  
46  
47  
48  
49  
50  
51  
52  
53  
54  
55  
56  
57  
58  
59  
60

**3-(4-(ethoxymethyl)-1H-1,2,3-triazol-1-yl)-N-(4-isopropylphenyl)benzenesulfonamide (17):**

Purification eluent EP/EA 7:3. White solid, Yield: 71% <sup>1</sup>H NMR: (400 MHz, CDCl<sub>3</sub>) δ 8.07 (s, 1H), 7.98 (t, *J*=8.4Hz, 1H), 7.79 (d, *J*=8.0Hz, 1H), 7.61, (t, *J*=8.0 Hz, 1H), 7.55 (s, 1H) 7.12 (d, *J*=8.0 Hz, 2H), 7.25 (s, 1H), 7.05 (d, *J*=8.4 Hz, 2H), 4.69 (s, 2H), 3.66-3.60 (m, 2H), 2.87-2.78 (m, 1H), 1.27 (t, *J*=7.2 Hz, 3H), 1,19 (d, *J*=6.8 Hz, 6H) ppm. <sup>13</sup>C NMR (100MHz, CDCl<sub>3</sub>-*d*) δ 147.08, 141.22, 138.37, 137.35, 134.97, 133.40, 130.61, 129.60, 127.44, 127.14, 124.49, 122.99, 120.61, 118.86,66.44, 64.06, 33.31, 24.10 (2C), 15.28 ppm. HRMS (ESI) *m/z* calcd for C<sub>20</sub>H<sub>23</sub>N<sub>4</sub>O<sub>3</sub>S [M-H]<sup>-</sup> 399.1491 found 399.1488.

**3-(4-butyl-1H-1,2,3-triazol-1-yl)-N-(4-methoxyphenyl)benzenesulfonamide (18).**

(Purification Eluent: Hexane-AcOEt 3:1). Yield 79%. <sup>1</sup>H NMR (400 MHz, CDCl<sub>3</sub>-*d*): δ 8.10 (s, 1H), 7.95-7.93 (d, *J*= 7.6 Hz, 1H), 7.71 (s, 1H), 7.68-7.66 (d, *J*= 7.7 Hz, 1H), 7.61 (s, 1H), 7.56-7.52 (t, *J*=7.9 Hz, 1H), 7.07-7.04 (d, *J*= 8.2Hz, 2H), 6.77-6.75 (d, *J*=8.2Hz, 2H), 3.73 (s, 3H), 2.78-2.75 (t, *J*= 7.7Hz, 2H), 1.71-1.64 (m, 2H), 1.43-1.36 (m, 2H), 0.95-0.91 (t *J*= 7.6Hz, 3H) ppm. <sup>13</sup>C NMR (100 MHz, MeOD-*d*<sub>4</sub>): δ 158.45, 149.70, 141.20, 137.55, 130.75, 127.59, 125.89 (2C), 124.43, 119.27, 118.89, 118.68, 114.46(2C), 55.90, 31.84, 25.52, 21.87, 13.85 ppm. HRMS (ESI) *m/z* calcd for C<sub>19</sub>H<sub>21</sub>N<sub>4</sub>O<sub>3</sub>S [M-H]<sup>-</sup> 385.1334 found 385.1338.

**3-(4-butyl-1H-1,2,3-triazol-1-yl)-N-(2-methoxyphenyl)benzenesulfonamide (19):**

(Purification eluent: Hexane-AcOEt 4:1). Yield 64% <sup>1</sup>H NMR (400 MHz, CDCl<sub>3</sub>) δ 8.28 (s, 1H), 8.08 (s, 1H), 7.97 (s, 1H), 7.62-7.60 (d, *J* = 8.0 Hz, 2H), 7.28-7.25 (t, *J* = 8.0 Hz, 1H), 6.68-6.65 (m, 4H), 3.80 (s, 3H), 2.78-2.73 (t, *J* = 8.0 Hz, 2H), 1.68-1.64 (m, 2H), 1.44 – 1.39 (m, 2H), 1.02 – 0.97 (m, 3H). <sup>13</sup>C NMR(100 MHz, CDCl<sub>3</sub>) δ 149.27, 149.11, 139.90, 139.74, 128.46, 127.64, 126.49, 124.93, 123.87, 123.11, 119.85, 119.72, 119.16, 114.93, 74.56, 31.00, 24.41, 21.46, 12.91.ppm. HRMS (ESI) *m/z* calcd for C<sub>19</sub>H<sub>21</sub>N<sub>4</sub>O<sub>3</sub>S [M-H]<sup>-</sup> 385.1334 found 385.1329.

1  
2  
3 **3-(4-butyl-1H-1,2,3-triazol-1-yl)-N-phenylbenzenesulfonamide (20):** (Purification eluent:  
4 Hexane-AcOEt 3:1). Yield 89%. <sup>1</sup>H NMR (400MHz, Acetone): δ 8.51 (s,1H), 8.08 (s, 1H), 7.88  
5  
6 – 7.74 (m, 2H), 7.69 (m, 1H), 7.45 (t, *J* = 7.9 Hz, 1H), 7.11 (t, *J* = 7.9 Hz, 2H), 6.90 – 6.79 (m,  
7  
8 1H), 6.60 (d, *J* = 7.5Hz, 2H), 2.76 (t, *J* = 7.8 Hz, 2H), 1.70 (t, *J* = 7.9Hz, 2H), 1.53–1.37 (m, 2H),  
9  
10 0.98 (t, *J* = 6.6 Hz, 3H)ppm. <sup>13</sup>C NMR (100 MHz, Acetone): 153.56, 141.73, 137.53, 137.00,  
11  
12 129.89, 129.42(2C), 128.59, 126.40, 125.09, 123.98, 121.69 (2C), 119.95, 29.99, 27.98, 22.18,  
13  
14 14.05ppm. HRMS (ESI) *m/z* calcd for C<sub>18</sub>H<sub>19</sub>N<sub>4</sub>O<sub>2</sub>S [M-H]<sup>-</sup> 355.1229 found 355.1224.  
15  
16  
17  
18

19 **4-(3-nitrophenyl)morpholine (23):** To a solution of 1-fluoro-3-nitrobenzene (1.0g, 7.1mmol)  
20  
21 in DMSO K<sub>2</sub>CO<sub>3</sub> (2.930 g,21.24 mmol) and morpholine (741mg, 8.5mmol) were added. The  
22  
23 solution was stirred at 60 °C for 3h. After this time 5% LiCl(aq) was added, and the reaction  
24  
25 mixture extracted with EtOAc (3x25mL) and dried over Na<sub>2</sub>SO<sub>4</sub>. The solvent was removed at  
26  
27 reduced pressure and the residue purified by flash chromatography on silica gel. Purification  
28  
29 Eluent PE/EA 8:2, Yield:80%. <sup>1</sup>H NMR (400 MHz, CDCl<sub>3</sub>) δ 7.72 (d, *J*=8.0 Hz, 1H), 7.43 (t,  
30  
31 *J*=8.0 Hz, 1H), 7.26 (s, 1H), 7.22 (d, *J*=6.4Hz, 1H) 3.90 (t, *J*=4.8 Hz, 4H) 3.27 (t, *J*=5.2 Hz, 4H)  
32  
33 ppm  
34  
35  
36  
37  
38

39 **3-morpholinoaniline (24):** **23** (500mg, 2.5 mmol) was solubilized in 30 mL of anhydrous  
40  
41 MeOH, to this Palladium on charcoal (50 mg) was added. The reaction mixture was stirred under  
42  
43 Hydrogen atmosphere for 1h, then the mixture was filtered off on a celite pad, the solvent  
44  
45 evaporated at reduced pressure and the residue purified by flash chromatography on silica gel.  
46  
47 Purification Eluent PE/EA= 8:2. Yield 99%.<sup>1</sup>H NMR: <sup>1</sup>H NMR: (400 MHz, CDCl<sub>3</sub>) δ 7.05 (t,  
48  
49 *J*=7.2 Hz, 1H), 6.37 (d, *J*=8.0 Hz, 1H), 6.25-6.20 (m, 2H), 4.24 (s, 2H), 3.19 (m, 4H), 2.6 (t,  
50  
51 *J*=4.4 Hz, 4H) ppm.  
52  
53  
54  
55  
56  
57  
58  
59  
60

1  
2  
3 ***N*-(2-trifluoromethyl)-3-nitro-phenylbenzenesulfonamide (28)**. To a stirred solution of 2-  
4 (trifluoromethyl)aniline (1.09 g, 6.76mmol) in 5 mL of anhydrous pyridine, was added the  
5  
6 corresponding 3-nitrobenzene sulfonyl chloride (1.5 g, 6.76 mmol) at 0°C. The corresponding  
7  
8 solution was stirred at r.t. under nitrogen atmosphere, for 5h. After completion of the reaction the  
9  
10 mixture was acidified with 20 mL of 2N HCl, the aqueous phase was extracted with several  
11  
12 times and the combined organic phases were dried (Na<sub>2</sub>SO<sub>4</sub>) and concentrated. The residue was  
13  
14 purified by flash chromatography on silica gel (Hexane-AcOEt 3:1). Yield 84%. <sup>1</sup>H NMR (400  
15  
16 MHz CDCl<sub>3</sub>-*d*): δ 8.56 (s, 1H), 8.40-8.38 (d, *J*=8.4 Hz, 1H), 8.06-8.04 (d, *J*=8 Hz, 1H), 7.86-  
17  
18 7.84 (d, *J*=8 Hz, 1H), 7.69-7.64 (t, *J*=8 Hz, 1H), 7.61-7.57 (t, *J*=7.8 Hz, 1H), 7.52-7.50 (d, *J*=8.0  
19  
20 Hz, 1H), 7.31-7.27 (t, *J*=8.1 Hz, 1H), 6.86 (s, 1H). MS (ESI): *m/z* 346.8 [M+H]<sup>+</sup>.  
21  
22  
23  
24  
25

26 **3-amino-N-(2-(trifluoromethyl)phenyl)benzenesulfonamide (29)** Sulfonamide **28** (400 mg,  
27  
28 1.35 mmol) was solubilized in 20 mL of anhydrous EtOH, and Palladium on charcoal (60 mg)  
29  
30 was added. The reaction mixture was stirred under Hydrogen atmosphere for 1h. Then the  
31  
32 mixture was filtered-off on a celite pad, was concentrated *in vacuo* and the crude product was  
33  
34 purified by flash chromatography on silica gel (Purification eluent: Hexane-AcOEt 3:1). Yield  
35  
36 84%. <sup>1</sup>H NMR (Acetone): δ 7.63-7.61 (d, *J*=8 Hz, 1H), 7.51-7.58 (m, 2H), 7.24-7.20 (t, *J*=8 Hz,  
37  
38 1H), 7.19-7.17 (m, 3H), 7.07-7.05 (d, *J*=8 Hz, 1H), 6.90-6.88 (d, *J*=8 Hz, 1H), 4.91 (s, 2H). MS  
39  
40 (ESI): *m/z* 338.8 [M+Na]<sup>+</sup>.  
41  
42  
43  
44  
45  
46

47 **3-azido-N-(2-(trifluoromethyl)phenyl)benzenesulfonamide (30)**. **29** (100 mg, 0.41 mmol) was  
48  
49 dissolved in CH<sub>3</sub>CN and cooled to 0°C in an ice-salt bath. To this stirred solution, tBuONO (225  
50  
51 μL, 1.89 mmol) was added, and the mixture was stirred for 10 min, after this time, TMSN<sub>3</sub> (200  
52  
53 μL, 1.52 mmol) was added dropwise, during 10 minutes, and the resulting brown solution was  
54  
55  
56  
57  
58  
59  
60

1  
2  
3 stirred at r.t. One hour later the solvent was removed at reduced pressure and the residue was  
4  
5 purified by flash chromatography on silica gel with the appropriate eluent. (Purification eluent:  
6  
7 Hexane-AcOEt 4:1).  $^1\text{H}$  NMR (400 MHz  $\text{CDCl}_3$ -d):  $\delta$  7.84-7.81 (d,  $J=8.4$  Hz, 1H), 7.56-7.50 (m,  
8  
9 3H), 7.43-7.37 (m, 2H), 7.27-7.23 (t,  $J=7.6$  Hz, 1H), 7.18- 7.16 (d,  $J= 8$ Hz, 1H), 6.87 (s, 1H)  
10  
11 ppm. MS (ESI): m/z 364.8  $[\text{M}+\text{Na}]^+$ .  
12  
13  
14  
15  
16

17 *General procedure for the preparation of compounds 31-34.*  
18

19 The appropriate alkyne (6.08 mmol) and the opportune azide (5.07 mmol) were suspended in a  
20  
21 1:1 mixture of water and *t*-BuOH (1.5 mL each) in a 10 mL glass vial equipped with a small  
22  
23 magnetic stirring bar. To this, sodium ascorbate (2.5 mmol) and copper(II) sulfate pentahydrate  
24  
25 (2.50 mmol) were added. The mixture was then heated for 10 min. at 125°C under microwave  
26  
27 irradiation, using an irradiation power of 300W. After that time the solvent was removed at  
28  
29 reduced pressure water was added and the mixture was extracted with EtOAc (3x 20 mL). The  
30  
31 organic layers were collected, washed with Brine and dried over  $\text{Na}_2\text{SO}_4$ . The crude was purified  
32  
33 by flash chromatography on silica gel using the opportune eluent to give the desired triazole  
34  
35 compounds **31-34**.  
36  
37  
38  
39  
40

41 **3-(4-isopentyl-1H-1,2,3-triazol-1-yl)-N-(2 (trifluoromethyl)phenyl) benzene sulfonamide**  
42

43 **(31)**: (Purification eluent: PE/EtOAc 7:2) ,Yield 69%, yellow solid.  $^1\text{H}$  NMR ( $\text{CDCl}_3$ ):  $\delta$  8.06 (s,  
44  
45 1H), 8.01-8.00 (d,  $J= 7.6$  Hz, 1H), 7.84-7.82 (d,  $J=8.0$  Hz, 1H), 7.76-7.74 (d,  $J= 7.6$  Hz, 1H),  
46  
47 7.69 (1H, s), 7.60-7.56 (t,  $J= 8.4$  Hz, 1H), 7.53-7.49 (m, 2H), 7.27-7.25 (d,  $J= 8.0$  Hz, 1H), 6.98  
48  
49 (s, 1H), 2.80-2.78 (m, 2H), 1.62 (m, 3H), 0.99-0.94 (m, 6H)ppm.  $^{13}\text{C}$  NMR ( $\text{CDCl}_3$ ):  $\delta$  149.95,  
50  
51 143.95, 137.71, 136.51, 133.39, 130.71, 130.14, 128.54, 126.68, 126.01, 125.29, 124.91, 124.15,  
52  
53  
54  
55  
56  
57  
58  
59  
60

1  
2  
3 121.56(q,  $J(\text{C-F})=270\text{Hz}$ ), 118.51, 38.27, 27.62, 23.51, 22.36 (2C) ppm. HRMS (ESI)  $m/z$  calcd  
4 for  $\text{C}_{20}\text{H}_{20}\text{F}_3\text{N}_4\text{O}_2\text{S}$   $[\text{M-H}]^-$  437.1259 found 437.1255.  
5  
6  
7  
8  
9

10  
11 **3-(4-cyclohexyl-1H-1,2,3-triazol-1-yl)-N-(2 (trifluoromethyl)phenyl) benzene sulfonamide**

12  
13 **(32):** (Purification eluent: PE/EtOAc 7:3), Yield 71%, pale white solid.  $^1\text{H}$  NMR ( $\text{CDCl}_3$ ):  $\delta$  8.39  
14 (s, 1H), 8.35 (s, 1H), 8.18-8.16 (d,  $J = 7.8$  Hz, 1H), 7.87-7.85 (d,  $J = 7.8$  Hz, 1H), 7.80-7.76 (t,  $J$   
15 = 7.8 Hz, 1H), 7.68-7.66 (d,  $J = 7.8$  Hz, 1H), 7.63-8.60 (m, 2H), 7.52-7.50 (d,  $J = 7.8$  Hz, 1H),  
16 7.44-7.40 (t,  $J = 8.0$  Hz, 1H), 3.47-3.41 (m, 1H), 2.51-2.37 (m, 4H), 1.80-1.63 (m, 6H).  $^{13}\text{C}$   
17 NMR ( $\text{CDCl}_3$ ):  $\delta$  149.31, 141.73, 138.07 (q,  $J(\text{C-F})=32\text{Hz}$ ), 137.00, 134.84, 123.37, 128.55,  
18 128.22, 127.57, 127.48, 127.07, 126.24, 123.95, 123.67(q,  $J(\text{C-F})=270\text{Hz}$ ), 119.92, 37.20,  
19 32.15(2C), 25.92, 25.15(2C). ppm. HRMS (ESI)  $m/z$  calcd for  $\text{C}_{21}\text{H}_{20}\text{F}_3\text{N}_4\text{O}_2\text{S}$   $[\text{M-H}]^-$  449.1259  
20 found 449.1262  
21  
22  
23  
24  
25  
26  
27  
28  
29  
30

31  
32  
33 **3-(4-ethyl-1H-1,2,3-triazol-1-yl)-N-(2 (trifluoromethyl)phenyl) benzene sulfonamide (33):**

34  
35 (Purification eluent: PE/EtOAc 7:2), Yield 78%, white solid.  $^1\text{H}$  NMR ( $\text{CDCl}_3$ ):  $\delta$  8.77 (s, 1H),  
36 8.40 (s, 1H), 8.35 (s, 1H), 8.17-8.15 (d,  $J = 7.6$  Hz, 1H), 7.88-7.86 (d,  $J = 7.6$  Hz, 1H), 7.81-7.77  
37 (t,  $J = 8.0$  Hz, 1H), 7.69-7.67 (t,  $J = 8.0$  Hz, 1H), 7.64-7.60 (t,  $J = 8.0$  Hz, 1H), 7.52-7.50 (d,  $J = 8.0$   
38 Hz, 1H), 7.45-7.41 (t,  $J = 8.0$  Hz, 1H), 2.76-2.78 (q,  $J = 7.6$  Hz, 2H), 1.30-1.26 (t,  $J = 7.6$  Hz,  
39 3H) ppm.  $^{13}\text{C}$  NMR ( $\text{CDCl}_3$ ):  $\delta$  149.1, 142.76, 137.94, 134.22, 133.37, 130.97, 127.47, 126.97,  
40 126.37, 125.31, 124.80, 123.87, 121.89 (q,  $J(\text{C-F})=270\text{Hz}$ ), 119.26(m), 118.29(m), 18.75, 12.92  
41 ppm. HRMS (ESI)  $m/z$  calcd for  $\text{C}_{17}\text{H}_{14}\text{F}_3\text{N}_4\text{O}_2\text{S}$   $[\text{M-H}]^-$  395.0790 found 395.0787  
42  
43  
44  
45  
46  
47  
48  
49  
50

51  
52 **3-(4-phenyl-1H-1,2,3-triazol-1-yl)-N-(2 (trifluoromethyl)phenyl) benzene sulfonamide (34):**

53  
54 (Purification eluent: PE/EtOAc 7:2), Yield 78%, yellow solid.  $^1\text{H}$  NMR ( $\text{CDCl}_3$ ):  $\delta$  9.09 (s, 1H),  
55  
56  
57  
58  
59  
60

1  
2  
3 8.82 (s, 1H), 8.44 (s, 1H), 8.28-8.26 (d,  $J=7.6$  Hz, 1H), 7.99-7.97 (d,  $J=8.0$  Hz, 2H), 7.94-7.92  
4 (d,  $J=7.6$  Hz, 1H), 7.86-7.82 (t,  $J=7.6$  Hz, 1H), 7.70-7.68 (d,  $J=8.1$  Hz, 1H), 7.65-7.61 (t,  $J=$   
5 7.6 Hz, 1H), 7.55-7.53 (t,  $J=8.0$  Hz, 1H), 7.48-7.42 (m, 3H), 7.36-7.34 (t,  $J=8.0$  Hz, 1H)ppm.  
6  
7  
8  
9  
10  $^{13}\text{C}$  NMR ( $\text{CDCl}_3$ ):  $\delta$  148.29, 142.80, 137.76, 134.10, 133.37, 131.09, 130.54, 129.00 (2C),  
11  
12 128.82, 128.45, 127.63, 127.40, 126.96, 126.74, 125.66(2C), 124.94, 124.14(m), 121.90,  
13  
14 118.84(q,  $J(\text{C-F})=30.3\text{Hz}$ ), ppm. HRMS (ESI)  $m/z$  calcd for  $\text{C}_{21}\text{H}_{14}\text{F}_3\text{N}_4\text{O}_2\text{S}$   $[\text{M-H}]^-$  443.0790  
15  
16 found 443.0793  
17  
18  
19

20 **4-(4-butyl-1H-1,2,3-triazol-1-yl)-N-(2-(trifluoromethyl)phenyl)benzenesulfonamide (35).**

21 (Purification eluent: Hexane-AcOEt 3:1). Yield 93%.  $^1\text{H}$  NMR (400 MHz,  $\text{CDCl}_3-d$ ):  $\delta$  8.89-  
22 7.81 (m, 5H) 7.75 (s, 1H), 7.57-7.53 (t,  $J=8.0$  Hz, 1H), 7.51-7.49 (d,  $J=8.0$  Hz, 1H), 7.26-7.22  
23 (m 1H), 6.94, (s, 1H), 2.79-2.75 (t,  $J=7.4$  Hz, 2H), 1.73-1.65 (m, 2H), 1.43-1.36 (m, 2H), 0.95-  
24 0.91 (t,  $J=8.0$  Hz, 3H) ppm.  $^{13}\text{C}$  NMR (100 MHz,  $\text{CDCl}_3-d$ ): 149.9, 140.8, 137.99, 133.88,  
25 133.81, 133.56, 129.53 (2C), 126.71 (q,  $J(\text{C-F})=4.4\text{Hz}$ ), 125.70, 123.89, 122.27(q,  $J(\text{C-}$   
26 F)=274Hz), 120.88 (2C), 118.45, 31.32, 25.24, 22.24, 13.76 ppm. HRMS (ESI)  $m/z$  calcd for  
27  $\text{C}_{19}\text{H}_{18}\text{F}_3\text{N}_4\text{O}_2\text{S}$   $[\text{M-H}]^-$  423.1103 found 423.1107.  
28  
29  
30  
31  
32  
33  
34  
35  
36  
37

38 **4-nitro-N-(2-(trifluoromethyl)phenyl)benzenesulfonamide.** The residue was purified by flash  
39 chromatography on silica gel (Hexane-AcOEt 3:1). Yield 84%.  $^1\text{H}$  NMR (400 MHz Acetone- $d_6$ ):  
40  $\delta$  8.82 (s, 1H), 8.27-8.25 (d,  $J=8.0$  Hz, 2H), 7.91-7.89 (d,  $J=8.0$  Hz, 1H), 7.87-7.85 (d,  $J=8.0$  Hz,  
41 2H), 7.61-7.57 (t,  $J=8.0$  Hz, 1H), 7.53-7.51 (d,  $J=8.0$  Hz, 1H), 7.32-7.25 (t,  $J=8$  Hz, 1H) ppm.  
42  
43  
44  
45  
46  
47 MS:  $m/z$  345.8  $[\text{M-H}]^-$   
48  
49

50 **4-amino-N-(2-(trifluoromethyl)phenyl)benzenesulfonamide.** (Purification eluent: Hexane-  
51 AcOEt 2:1). Yield 97%.  $^1\text{H}$  NMR (Acetone- $d_6$ ):  $\delta$  7.89 (s, 1H), 7.53-7.51 (d,  $J=8.0$  Hz, 2H), 7.49-  
52  
53  
54  
55  
56  
57  
58  
59  
60

7.47 (d,  $J=8.0$  Hz, 1H), 7.45-7.43 (d,  $J=8$  Hz, 2H), 7.30-7.28 (t,  $J= 8$ Hz, 1H), 6.62-6.60 (t,  $J=7.8$  Hz, 1H), 6.50 (d,  $J=8.0$  Hz, 1H), 4.62 (s, 2H),. MS (ESI):  $m/z$  338.8  $[M+Na]^+$ .

**4-azido-N-(2-(trifluoromethyl)phenyl)benzenesulfonamide.** (Purification eluent: Hexane-AcOEt 4:1).  $^1H$  NMR (400 MHz  $CDCl_3-d$ ):  $\delta$  7.81-7.79 (m, 2H), 7.74-7.71 (d,  $J= 7.4$ Hz, 1H), 7.52-7.46 (m, 2H), 7.22-7.18 (t,  $J= 8$  Hz, 1H),7.02-6.98 (m, 3H) ppm.  $m/z$  364.7  $[M+Na]^+$ .

**N-(2-hydroxyphenyl)-4-nitrobenzenesulfonamide .**  $^1H$  NMR (Acetone- $d_6$ ):  $\delta$  8.25-8.22 (d,  $J= 8.4$  Hz 2H,),  $\delta$  7.93-7.91 (m, 3H), 7.33-7.31 (m, 2H), 6.97-6.94 (t,  $J= 7.6$  Hz, 1H), 6.76-6.73 (t,  $J= 7.6$  Hz, 1H), 6.66-6.64 (d,  $J= 8$  Hz,1 H) ppm. MS:  $m/z$  292.8  $[M-H]^-$

**4-amino-N-(2-hydroxyphenyl)benzenesulfonamide:**  $^1H$  NMR (Acetone- $d_6$ ):  $\delta$  7.55-7.53 (d,  $J= 8.0$  Hz, 2H), 7.42-7.40 (d,  $J= 8.0$  Hz, 2H), 7.22-7.18 (m, 1H,), 6.90-6.84 (m, 2H), 6.70-6.66 (m, 2H), 6.55-6.53 (d,  $J= 8.8$  Hz, 1H) ppm. MS:  $m/z$  265.0  $[M+H]^+$ .

**4-azido-N-(2-hydroxyphenyl)benzenesulfonamide:** (Purification eluent: Hexane-AcOEt 3:1).

$^1H$  NMR (MeOD- $d_4$ ):  $\delta$  7.73-7.72 (d,  $J= 8.0$  Hz, 2H), 7.36-7.35 (d,  $J= 6.4$  Hz, 1H), 7.09-7.07 (d,  $J= 8.0$  Hz, 2H), 6.94-6.90 (m, 2H), 6.73-6.66 (m, 2H) ppm. MS:  $m/z$  312.8  $[M+Na]^+$

**4-(4-butyl-1H-1,2,3-triazol-1-yl)-N-(2-hydroxyphenyl)benzenesulfonamide (36).**

(Purification eluent: Hexane-AcOEt 4:1). Yield 80%  $^1H$  NMR (400 MHz, MeOD- $d_4$ ):  $\delta$  8.34 (s, 1H), 7.93-7.87 (m, 4H), 7.33-7.31 (d,  $J= 6.8$  Hz, 1H), 6.96-6.92 (m, 1H), 6.76-7.73 (t,  $J= 7.6$  Hz, 1H), 6.67-6.65 (d,  $J= 8.0$  Hz, 1H), 2.78-2.74 (t,  $J=7.6$  Hz, 2H) 1.74-1.66 (m, 2H), 1.45-1.36 (m, 2H), 1.27-1.22 (t,  $J=7.2$  Hz, 3H) ppm.  $^{13}C$  NMR (100 MHz, MeOD- $d_4$ ):  $\delta$  150.25, 149.21, 139.89, 139.78, 128.89(2C), 126.49, 124.93, 123.87, 119.85, 119.55 (2C), 119.16, 114.93, 30.99, 24.39, 21.44, 12.89.ppm. HRMS (ESI)  $m/z$  calcd for  $C_{18}H_{19}N_4O_3S$   $[M-H]^-$  371.1178 found 371.1173.

## II. Assays

### Enzymatic assays

#### *Protein expression and purification*

Recombinant his-tagged human full length DDX3X was cloned the *E. coli* expression vector pET-30a(+). ShuffleT7 *E. coli* cells were transformed with the plasmid and grown at 37°C up to OD<sub>600</sub> = 0.7. DDX3X expression was induced with 0.5 mM IPTG at 15°C O/N. Cells were harvested by centrifugation, lysed and the crude extract centrifuged at 100.000xg for 60 min at 4°C in a Beckman centrifuge before being loaded onto a FPLC Ni-NTA column (GE Healthcare). Column was equilibrated in Buffer A (50 mM Tris-HCl pH 8.0, 250 mM NaCl, 25 mM Imidazole and 20% glycerol). After extensive washing in Buffer A, the column was eluted with a linear gradient in Buffer A from 25 mM to 250 mM Imidazole. Proteins in the eluted fractions were visualized on a SDS-PAGE and tested for the presence of DDX3X by Western blot with anti-DDX3X A300-A450 (*BETHYL*) at 1:2000 dilution in 5% milk. Fractions containing the purest DDX3X protein were pooled and stored at -80°C.

#### *Helicase assay based on Fluorescence Resonance Energy Transfer (FRET)*

The dsRNA substrate for the helicase assay was prepared by hybridizing two ss RNA oligonucleotides with the following sequences:

Fluo-FAM 5' UUUUUUUUUUUUUUUAGUACCGCCACCCUCAGAACC 3'

Qu-BHQ1 5' GGUUCUGAGGGUGGCGGUACUA 3'

DNA capture 5' TAGTACCGCCACCCTCAGAACC 3'

1  
2  
3 The sequence in Fluo-FAM complementary to Qu-BHQ1 is underlined. Fluo-FAM carries a 6-  
4 carboxyfluorescein fluorophore at its 3' end, while Qu-BHQ1 carries a Black Hole quencher  
5 group at its 5' end. The DNA capture oligonucleotide is complementary to the Qu-BHQ1  
6 oligonucleotide, but bears no modifications.  
7  
8  
9  
10

11  
12  
13 Helicase assay using the dsRNA substrate was performed in 20mM TrisHCl (pH 8), 70 mM KCl,  
14 2mM MgCl<sub>2</sub>, 2mM dithiothreitol, 12 units RNasin, 2 mM ATP, 50 nM dsRNA and 100 nM  
15 capture strand in 20μl of reaction volume. The unwinding reaction was started by adding 60  
16 pmols of DDX3X recombinant protein and carried out at 37°C for 40 min using a LightCycler  
17 480 (Roche). The fluorescence intensity was recorded every 30 s. Data of fluorescence signal  
18 were analyzed by linear interpolation and the corresponding slope values were used to determine  
19 the apparent unwinding rate.  
20  
21  
22  
23  
24  
25  
26  
27  
28  
29

### 30 31 *Kinetic analysis*

32  
33  
34 The IC<sub>50</sub> values have been calculated from dose–response curves. Data (in triplicate) were  
35 plotted and analyzed by least-squares nonlinear regression, according to the method of  
36 Marquardt–Levenberg, with the computer program GraphPad Prism 6.0. Data were fitted to the  
37 following equation:  
38  
39  
40  
41  
42

$$43$$
$$44$$
$$45 \quad (1) \quad E_{\text{obs}} = E_{\text{max}} / (1 + (IC_{50}/[I])^n)$$
$$46$$

47  
48 where  $E_{(\text{obs})}$  is the observed enzymatic activity in the presence of each inhibitor dose [I];  $E_{(\text{max})}$  is  
49 the maximal enzymatic activity in the absence of the inhibitor;  $n$  is an exponential term to take  
50 into account sigmoidal dose–response curves.  
51  
52  
53  
54  
55  
56  
57  
58  
59  
60

### *Cell extracts and DDX3X quantification*

10<sup>7</sup> cells were ruptured with a Dounce homogenizer in Lysis Buffer (50 mM Tris HCl pH 8.0, 0.1% SDS, 350 mM NaCl, 0.25% Triton X-100, protease inhibitor cocktail (Sigma-Aldrich)). The lysate was incubated 30 min on ice, sonicated for 5 min (at 30 s intervals) and centrifuged at 15.000 x g for 10 min at 4°C. The protein concentration in the supernatant (crude extract) was quantified with Bradford. For DDX3X quantification, increasing concentrations of crude extract (5 μg, 10 μg, 20 μg, 40 μg) were loaded on a SDS-PAGE alongside known concentrations (50 ng, 100 ng, 150 ng, 200 ng) of recombinant purified DDX3X. Separated proteins were subjected to Western Blot analysis with anti-DDX3X A300-A450 (*BETHYL*) at 1:2000 dilution in 5% milk. The blot was next incubated with a HRP-conjugated secondary antibody and the bands corresponding to DDX3X were visualized with Enhanced Chemiluminescent Substrate (Westar Nova 2.0, Cyanagen) using a ChemiDoc™ XRS (Bio-Rad) apparatus. The intensity of the bands was measured by densitometry and the values obtained for the purified DDX3X were plotted as a function of the protein concentration and analyzed by linear interpolation to derive a reference curve, whose slope corresponded to the estimated intensity (I) x ng<sup>-1</sup> (DDX3X) value. This parameter was used to calculate the I x ng<sup>-1</sup> values for the DDX3X in the cell extract, from the intensities of the DDX3X bands in the corresponding cell extract (CE) samples. The mean I x ng<sup>-1</sup> (CE) value was used to calculate the ng of DDX3X x μL<sup>-1</sup> of extract, and then the total ng of DDX3X present in the extract. This value was divided for the total number of cells used (10<sup>7</sup>), to derive the ng DDX3X/cell. Based on the known molecular weight of DDX3X, the Avogadro number and assuming a mean cellular volume of 6.55 x 10<sup>-11</sup> L, the final molar concentration of DDX3X per cell was calculated. Each experiment was repeated three times, with each blot carrying a reference curve alongside the extract samples, to account for variations in

1  
2  
3 loading/transfer efficiency. The reference I x ng<sup>-1</sup> (DDX3X) value obtained was anyway  
4  
5 comparable across the different experiments ( $\pm 20\%$  variation).  
6  
7

#### 8 9 *ATPase assay*

10  
11  
12 The ATPase assay was carried out by using the commercial kit Promega ADP-Glo™ Kinase  
13  
14 Assay. Reaction was performed in 30mM TrisHCl, 9 mM MgCl<sub>2</sub>, 0.05mg/ml BSA, 50μM ATP  
15  
16 and 4μM DDX3. Reaction was performed following the ADP-Glo™ Kinase Assay Protocol and  
17  
18 luminescence was measured with MicroBeta TriLux Perkin Elemer.  
19  
20  
21  
22

23 The anti-DDX1 activity was evaluated as previously reported.<sup>29</sup>  
24  
25  
26  
27  
28  
29

#### 30 **Antiviral assay**

##### 31 32 33 **WNV inhibitory viral plaque reduction assay**

34  
35  
36  
37  
38 Huh7 cells, derived from human hepatoma (kindly provided from Istituto Toscano  
39  
40 Tumori, Core Research Laboratory, Siena, Italy) was used for the inhibitory viral plaque  
41  
42 reduction assay. The cell propagation medium was Dulbecco's Modified Eagle's  
43  
44 Medium (DMEM; SIGMA, Milano, Italy) supplemented with 10% Fetal Bovine Serum  
45  
46 (FBS; SIGMA) and 1% Penicillin/Streptomycin (SIGMA). WNV (strain of lineage 2) viral  
47  
48 stock, consisting of cell-free supernatants of acutely infected Huh7 cells, were aliquoted  
49  
50  
51  
52  
53  
54  
55  
56  
57  
58  
59  
60

1  
2  
3 and stored at  $-80^{\circ}\text{C}$  until used. Titration of the viral stocks as plaque forming unit (PFU)  
4  
5  
6  
7 was carried out in Huh7 cells. WNV was used to infect Huh7 cell line in duplicate and  
8  
9  
10 viral plaques were visualized 4 days following infection. Briefly, 6-well plates were  
11  
12  
13 seeded with  $2.5 \times 10^5$  cells in 3 mL of growth medium and kept overnight at  $37^{\circ}\text{C}$  with  
14  
15  
16  
17 5%  $\text{CO}_2$ . The day of infection, after removal of growth medium, cell monolayers at 80–  
18  
19  
20 90% confluence were infected with WNV viral stock with a multiplicity of infection (MOI)  
21  
22  
23 of 0.1 in a final volume of 0.3 mL and incubated for 1 h at  $37^{\circ}\text{C}$  with 5%  $\text{CO}_2$ . Then,  
24  
25  
26  
27 cells were washed with PBS 1X, and 30  $\mu\text{L}$  dimethylsulfoxide (DMSO) alone (viral  
28  
29  
30 positive control) or with 10-fold serial dilutions of DDX3X inhibitory compounds were  
31  
32  
33 immediately added in duplicates together with 300  $\mu\text{L}$  of fresh DMEM complete medium  
34  
35  
36  
37 (compound final concentrations of 100, 10, 1, 0.1, and 0.01  $\mu\text{M}$ ). Ribavirin (1- $\beta$ -d-  
38  
39  
40 Ribofuranosyl-1,2,4-Triazole-3-Carboxamide; SIGMA) diluted in DMSO was used as  
41  
42  
43 inhibitory reference control. Then, the overlay medium composed by 0.5% Sea Plaque  
44  
45  
46  
47 Agarose (Lonza, Basel, Switzerland) diluted in propagation medium was added to each  
48  
49  
50 well. After 4 days (Huh7) of incubation at  $37^{\circ}\text{C}$ , the monolayers were fixed with  
51  
52  
53  
54 methanol (Carlo Erba Chemicals, Milan, Italy) and stained with 0.1% crystal violet (Carlo  
55  
56  
57  
58  
59  
60

1  
2  
3 Erba Chemicals) and the viral titers were calculated by Plaque forming unit (PFU)  
4  
5  
6  
7 counting. Percent of Plaque reduction activity was calculated by dividing the average  
8  
9  
10 PFU of treated samples by the average of DMSO-treated samples (viral positive  
11  
12  
13 control). Fifty percent inhibitory concentrations ( $IC_{50}$ ) were calculated using the  
14  
15  
16 predicted exponential growth function in Microsoft Excel, which uses existing x-y data to  
17  
18  
19 estimate the corresponding anti DDX3X compound concentration (x) from a known  
20  
21  
22 value (y), which in this case was 50% PFU. Mean  $IC_{50} \pm$  standard deviations (SD) were  
23  
24  
25  
26 calculated using all replicates. All experiments were repeated at least twice. All  
27  
28  
29  
30  
31 experimental procedures were conducted under biosafety level 3 containment.  
32  
33

### 34 35 36 **Cytotoxicity assay**

37  
38  
39  
40 Monolayers of  $2.5 \times 10^4$  Huh7 cells per well in a flat-bottom 96-well culture plates and  
41  
42  
43 allowed to adhere overnight. Then, when the cell layers were confluent, the medium  
44  
45  
46 was removed, the wells were washed twice with PBS, treated with 100  $\mu$ l of DMEM with  
47  
48  
49 10  $\mu$ l DMSO alone (cell positive control) or with various concentrations of DDX3X  
50  
51  
52  
53 inhibitory compounds under study (compound final concentrations of 100, 10, 1, 0.1,  
54  
55  
56  
57  
58  
59  
60

1  
2  
3 and 0.01  $\mu\text{M}$ ) and incubated for 3 days at 37°C in a CO<sub>2</sub>. After treatment, an MTT (3-  
4  
5  
6  
7 (4,5-dimethylthiazol-2-yl)-2,5-diphenyltetrazolium bromide) kit (Roche, Milan, Italy) was  
8  
9  
10 used according to the supplier's instructions, and the absorbance of each well was  
11  
12  
13 determined using a microplate spectrophotometer at a wavelength of 570 nm.  
14  
15  
16  
17 Cytotoxicity was calculated by dividing the average optical density of treated samples by  
18  
19  
20 the average of DMSO-treated samples (cell positive control).  
21  
22  
23  
24

#### 25 **Virus RNA quantification and capsid protein detection assay**

26  
27  
28  
29 Total RNA was extracted and purified from infected and control cells using an RNAeasy  
30  
31  
32 mini Kit (Qiagen). Two hundred nanograms of total RNA of each sample in a 20  $\mu\text{l}$   
33  
34  
35  
36 reaction mixture were reverse-transcribed by using the indicated primers (primer PROCf  
37  
38  
39  
40 5' C C T g T g T g A g C T g A C A A A C T T A g T 3' for the transcription of WNV  
41  
42  
43  
44 complementar RNA and primer PROCr 5' g C g T T T T A g C A T A T T g A C A g  
45  
46  
47 C C 3' for the transcription of WNV genomic RNA) and amplified by real-time PCR in a  
48  
49  
50 Rotor-gene 3000 real-time thermal cycler (Corbett research, Australia) with the following  
51  
52  
53  
54 WNV specific primer and probe (primer PROCf 5' C C T g T g T g A g C T g A C A A  
55  
56  
57  
58  
59  
60

1  
2  
3 A C T T A g T 3' and primer PROCr 5' g C g T T T T A g C A T A T T g A C A g C

4  
5  
6  
7 C 3', and probe PROC-TMD VIC-5' CCTGGTTTCTTAGACATCGAGATCTTCGTGC

8  
9  
10 3')<sup>24</sup>. Plasmid calibration standards were used for quantification of template  
11  
12  
13  
14 concentration. The sensibility of the assay was 10 copies.

15  
16  
17  
18 The specific WNV capsid protein, was investigated with Western blot analysis of Huh7  
19  
20  
21  
22 infected cells electrophoresed on 10% SDS-PAGE and then probed with anti-capsid  
23  
24  
25  
26  
27  
28  
29 protein polyclonal antibody followed by peroxidase-conjugated anti-rabbit IgG polyclonal  
30  
31  
32  
33  
34  
35  
36  
37  
38  
39  
40  
41  
42  
43  
44  
45  
46  
47  
48  
49  
50  
51  
52  
53  
54  
55  
56  
57  
58  
59  
60 antibody.

### ADME assay

*Chemicals.* All solvents, reagents, were from Sigma-Aldrich Srl (Milan, Italy), Brain Polar Lipid Extract (Porcine) were from Avanti Polar Lipids, INC. (Alabama, USA). Dodecane was purchased from Fluka (Milan, Italy). Pooled Male Donors 20 mg/mL HLM were from BD Gentest-Biosciences (San Jose, California). Milli-Q quality water (Millipore, Milford, MA, USA) was used. Hydrophobic filter plates (MultiScreen-IP, Clear Plates, 0.45  $\mu\text{m}$  diameter pore size), 96-well microplates, and 96-well UV-transparent microplates were obtained from Millipore (Bedford, MA, USA).

*Parallel artificial membrane permeability assay (PAMPA and PAMPA-BBB).* Donor solution (0.5 mM) was prepared by diluting 1 mM dimethylsulfoxide (DMSO) compound stock solution using phosphate buffer (pH 7.4, 0.025 M). Filters were coated with 5  $\mu\text{L}$  of a 1% (w/v) dodecane solution of phosphatidylcholine or 4  $\mu\text{L}$  of brain polar lipid solution (20 mg/mL 16%  $\text{CHCl}_3$ , 84% dodecane) prepared from  $\text{CHCl}_3$  solution 10% w/v, for intestinal permeability and BBB permeability, respectively. Donor solution (150  $\mu\text{L}$ ) was added to each well of the filter plate. To each well of the acceptor plate were added 300  $\mu\text{L}$  of solution (50% DMSO in phosphate buffer). All compounds were tested in three different plates on different days. The sandwich was incubated for 5 h at room temperature under gentle shaking. After the incubation time, the plates were separated, and samples were taken from both receiver and donor sides and analyzed using LC with UV detection at 280 nm. LC analysis were performed with a PerkinElmer (series 200) instrument equipped with an UV detector (PerkinElmer 785A, UV/vis Detector). Chromatographic separation were conducted using a Polaris C18 column (150 - 4.6 mm, 5  $\mu\text{m}$  particle size) at a flow rate of 0.8  $\text{mL min}^{-1}$  with a mobile phase composed of 60% ACN/40%

H<sub>2</sub>O-formic acid 0.1% for all compounds. Permeability ( $P_{app}$ ) were calculated according to the following equation with some modification in order to obtain permeability values in cm/s,

$$P_{app} = \frac{V_D V_A}{(V_D + V_A) A t} - \ln(1 - r)$$

where  $V_A$  is the volume in the acceptor well,  $V_D$  is the volume in the donor well (cm<sup>3</sup>),  $A$  is the “effective area” of the membrane (cm<sup>2</sup>),  $t$  is the incubation time (s) and  $r$  the ratio between drug concentration in the acceptor and equilibrium concentration of the drug in the total volume ( $V_D + V_A$ ). Drug concentration is estimated by using the peak area integration. Membrane retentions (%) were calculated according to the following equation:

$$\%MR = \frac{[r - (D + A)]100}{Eq}$$

where  $r$  is the ratio between drug concentration in the acceptor and equilibrium concentration,  $D$ ,  $A$ , and  $Eq$  represented drug concentration in the donor, acceptor and equilibrium solution, respectively.

*Water solubility assay.* Compound **1** (1 mg) was added to 1 mL of water. The sample was shaken in a shaker bath at room temperature for 24-36 h. The suspensions were filtered through a 0.45 μm nylon filter (Acrodisc), and the solubilized compound determined by LC-MS-MS assay. The determination was performed in triplicate. For the quantification was used an LC-MS system

1  
2  
3 consisted of a Varian apparatus (Varian Inc) including a vacuum solvent degassing unit, two  
4 pumps (212-LC), a Triple Quadrupole MSD (Mod. 320-LC) mass spectrometer with ES interface  
5 and Varian MS Workstation System Control Vers. 6.9 software. Chromatographic separation  
6 was obtained using a Pursuit C18 column (50 x 2.0 mm) (Varian) with 3  $\mu\text{m}$  particle size and  
7 gradient elution: eluent A being ACN and eluent B consisting of an aqueous solution of formic  
8 acid (0.1%). The analysis started with 0% of eluent A, which was linearly increased up to 70% in  
9 10 min, then slowly increased up to 98% up to 15 min. The flow rate was 0.3 mL/min and  
10 injection volume was 5  $\mu\text{L}$ . The instrument operated in positive mode and parameters were:  
11 detector 1850 V, drying gas pressure 25.0 psi, desolvation temperature 300.0  $^{\circ}\text{C}$ , nebulizing gas  
12 45.0 psi, needle 5000 V and shield 600 V. Nitrogen was used as nebulizer gas and drying gas.  
13 Collision induced dissociation was performed using Argon as the collision gas at a pressure of  
14 1.8 mTorr in the collision cell. Quantification of the single compound was made by comparison  
15 with apposite calibration curves realized with standard solutions in methanol.  
16  
17  
18  
19  
20  
21  
22  
23  
24  
25  
26  
27  
28  
29  
30  
31  
32  
33

34 *Microsomal stability assay.* Each compound in DMSO solution was incubated at 37  $^{\circ}\text{C}$  for 60  
35 min in 125 mM phosphate buffer (pH 7.4), 5  $\mu\text{L}$  of human liver microsomal protein (0.2  
36 mg/mL), in the presence of a NADPH-generating system at a final volume of 0.5 mL  
37 (compounds' final concentration, 50  $\mu\text{M}$ ); DMSO did not exceed 2% (final solution). The  
38 reaction was stopped by cooling in ice and adding 1.0 mL of acetonitrile. The reaction mixtures  
39 were then centrifuged, and the parent drug and metabolites were subsequently determined by  
40 LC-UV-MS. Chromatographic analysis were performed with an Agilent 1100 LC/MSD VL  
41 system (G1946C) (Agilent Technologies, Palo Alto, CA) constituted by a vacuum solvent  
42 degassing unit, a binary high-pressure gradient pump, an 1100 series UV detector, and an 1100  
43 MSD model VL benchtop mass spectrometer. Chromatographic separation was obtained using a  
44  
45  
46  
47  
48  
49  
50  
51  
52  
53  
54  
55  
56  
57  
58  
59  
60

1  
2  
3 Varian Polaris C18-A column (150 - 4.6 mm, 5  $\mu\text{m}$  particle size) and gradient elution: eluent A  
4 being ACN and eluent B consisting of an aqueous solution of formic acid (0.1%). The analysis  
5 started with 2% of eluent A, which was rapidly increased up to 70% in 12 min, then slowly  
6 increased up to 98% in 20 min. The flow rate was 0.8 mL  $\text{min}^{-1}$  and injection volume was 20  $\mu\text{L}$ .  
7  
8 The Agilent 1100 series mass spectra detection (MSD) single-quadrupole instrument was  
9 equipped with the orthogonal spray API-ES (Agilent Technologies, Palo Alto, CA). Nitrogen  
10 was used as nebulizing and drying gas. The pressure of the nebulizing gas, the flow of the drying  
11 gas, the capillary voltage, the fragmentor voltage, and the vaporization temperature were set at  
12 40 psi, 9 L/min, 3000 V, 70 V, and 350  $^{\circ}\text{C}$ , respectively. UV detection was monitored at 280 nm.  
13  
14 The LC-ESI-MS determination was performed by operating the MSD in the positive ion mode.  
15  
16 Spectra were acquired over the scan range  $m/z$  100-1500 using a step size of 0.1 u. The  
17 percentage of not metabolized compound was calculated by comparison with reference solutions.  
18  
19  
20  
21  
22  
23  
24  
25  
26  
27  
28  
29  
30

## 31 ASSOCIATED CONTENT

32 Supporting Information available:

33  
34  
35  
36  
37  
38  
39  
40 The Supporting Information is available free of charge on the ACS Publications website

41  
42  
43  
44 <http://pubs.acs.org>.

45  
46  
47  
48 Western blot experiments for the quantification of DDX3X in cell extracts, representative

49  
50  
51 IC50 curves, Anti-WNV dose-response and cytotoxicity curves (PDF).  
52  
53  
54  
55  
56  
57  
58  
59  
60

1  
2  
3  
4 Molecular formula strings (CSV).  
5  
6  
7

## 8 **AUTHOR INFORMATION**

9

### 10 11 12 **Corresponding Author**

13  
14  
15  
16 \* E-mail \*botta.maurizio@gmail.com (BM)  
17  
18  
19

### 20 21 **Author Contributions**

22  
23  
24 The manuscript was written through contributions of all authors. All authors have given  
25  
26  
27  
28 approval to the final version of the manuscript.  
29  
30  
31

## 32 **ACKNOWLEDGMENT**

33  
34

35 This work was supported by First Health Pharmaceuticals B. V. (Amsterdam) to MB. Financial  
36  
37 support has been also provided by Tuscany Region Grant FAS Salute 2014 (DD 4042/2014) to  
38  
39 MB and SG.  
40  
41  
42

## 43 **NOTES**

44

45  
46  
47 This paper is dedicated to the memory of Pier Giovanni Baraldi, emeritus Professor at the  
48  
49 University of Ferrara and beloved chemist.  
50  
51  
52

## 53 **ABBREVIATIONS**

54  
55  
56  
57  
58  
59  
60

1  
2  
3 West Nile Virus WNV; tert-Butyl nitrite (t-BuONO); absorption, distribution, metabolism  
4  
5  
6  
7 and excretion (ADME).  
8  
9

## 10 11 REFERENCES

- 12  
13  
14  
15  
16 [1] Caren Chancey, Andriyan Grinev, Evgeniya Volkova, and Maria Rios. The global  
17 ecology and epidemiology of West Nile Virus. *Biomed Res Int.* **2015**; 2015, 376230.  
18  
19 [2] European Centre for Disease Prevention and Control. (2018). Epidemiological update:  
20 West Nile virus transmission season in Europe, 2017. [online] Available at:  
21 [https://ecdc.europa.eu/en/news-events/epidemiological-update-west-nile-virus-](https://ecdc.europa.eu/en/news-events/epidemiological-update-west-nile-virus-transmission-season-europe-2017)  
22 [transmission-season-europe-2017](https://ecdc.europa.eu/en/news-events/epidemiological-update-west-nile-virus-transmission-season-europe-2017) [Accessed 22 Aug. 2018].  
23  
24 [3] Cdc.gov. (2018). Preliminary maps & data for 2017 | West Nile Virus | CDC. [online]  
25 Available at:  
26 <https://www.cdc.gov/westnile/statsmaps/preliminarymapsdata2017/index.html>  
27 [Accessed 22 Aug. 2018].  
28  
29 [4] European centre for disease prevention and control. (2018). Weekly updates: 2018 West  
30 Nile fever transmission season. [online] Available at: [https://ecdc.europa.eu/en/west-nile-](https://ecdc.europa.eu/en/west-nile-fever/surveillance-and-disease-data/disease-data-ecdc)  
31 [fever/surveillance-and-disease-data/disease-data-ecdc](https://ecdc.europa.eu/en/west-nile-fever/surveillance-and-disease-data/disease-data-ecdc) [Accessed 31 Aug. 2018].  
32  
33 [5] Caren Chancey, Andriyan Grinev, Evgeniya Volkova, and Maria Rios. The global  
34 ecology and epidemiology of West Nile virus. *Biomed Res Int.* **2015**; 2015, 376230.  
35  
36 [6] Wilder-Smith A, Gubler DJ, Weaver SC, Monath TP, Heymann DL, Scott TW. Epidemic  
37 arboviral diseases: priorities for research and public health. *Lancet Infect Dis.* **2017** 17,  
38 e101-e106.  
39  
40  
41  
42  
43  
44  
45  
46  
47  
48  
49  
50  
51  
52  
53  
54  
55  
56  
57  
58  
59  
60

- 1  
2  
3 [7] Mercorelli B, Palù G, Loregian A. Drug repurposing for viral infectious diseases: how far  
4 are we? *Trends Microbiol.* **2018** pii: S0966-842X(18)30087-8.  
5  
6  
7 [8] Valiente-Echeverría F, Hermoso MA, Soto-Rifo R. RNA helicase DDX3: at the  
8 crossroad of viral replication and antiviral immunity. *Rev Med Virol.* **2015**, 25, 286-299.  
9  
10 [9] Shuiping Chen, Harendra S. Chahar, Sojan Abraham, Haoquan Wu, Theodore C.  
11 Pierson, Xiaozhong A. Wang, and N. Manjunath. Ago-2-mediated slicer activity is  
12 essential for anti-flaviviral efficacy of RNAi. *PLoS One* **2011**, 6, e27551.  
13  
14 [10] Chahar HS, Chen S, Manjunath N. P-body components LSM1, GW182, DDX3,  
15 DDX6 and XRN1 are recruited to WNV replication sites and positively regulate viral  
16 replication. *Virology.* **2013** 436, 1-7.  
17  
18 [11] Owsianka AM, Patel AH Hepatitis C virus core protein interacts with a human  
19 DEAD box protein DDX3 *Virology*, **1999**, 257, 330–340  
20  
21 [12] Mamiya N, Worman HJ Hepatitis C virus core protein binds to a DEAD box  
22 RNA helicase *J Biol Chem*, **1999**, 274, 15751–15756.  
23  
24 [13] Ariumi Y, Kuroki M, Abe K, Dansako H, Ikeda M, Wakita T DDX3 DEAD-box  
25 RNA helicase is required for hepatitis C virus RNA replication *J Virol*, **2007**, 81, 13922–  
26 13926.  
27  
28 [14] Li C, Ge LL, Li PP, Wang Y, Dai JJ, Sun MX, Huang L, Shen ZQ, Hu XC, Ishag  
29 H, Mao Z, Cellular DDX3 regulates Japanese encephalitis virus replication by interacting  
30 with viral un-translated regions *Virology*, **2014**, 449, 70-81.  
31  
32 [15] Noble CG, Chen YL, Dong H, Gu F, Lim SP, Schul W, Wang QY, Shi PY  
33 Strategies for development of Dengue virus inhibitors. *Antiviral Research*, **2010**, 85,  
34 3450–3462.  
35  
36  
37  
38  
39  
40  
41  
42  
43  
44  
45  
46  
47  
48  
49  
50  
51  
52  
53  
54  
55  
56  
57  
58  
59  
60

- 1  
2  
3 [16] Benfield CT, Ren H, Lucas SJ, Bahsoun B, Smith GL Vaccinia virus protein K7  
4 is a virulence factor that alters the acute immune response to infection *J Gen Virol* **2013**,  
5 *94*, 1647-1657.  
6  
7  
8  
9  
10 [17] Tintori C., Brai A., Fallacara A. L., Fazi R., Schenone S., Botta M.. Protein-  
11 protein interactions and human cellular cofactors as new targets for HIV therapy. *Curr.*  
12 *Opin. Pharmacol.* **2014**, *18*, 1-8.  
13  
14  
15  
16  
17 [18] Radi M., Falchi F., Garbelli A., Samuele A., Bernardo V., Paolucci S., Baldanti  
18 F., Schenone S., Manetti F., Maga G., Botta M., Discovery of the first small molecule  
19 inhibitor of human DDX3 specifically designed to target the RNA binding site: towards  
20 the next generation HIV-1 inhibitors. *Bioorg. Med. Chem. Lett.* **2012**, *22*, 2094-2098.  
21  
22  
23  
24  
25 [19] Brai A, Fazi R, Tintori C, Zamperini C, Bugli F, Sanguinetti M, Stigliano E, Esté  
26 J, Badia R, Franco S, Martinez MA, Martinez JP, Meyerhans A, Saladini F, Zazzi M,  
27 Garbelli A, Maga G, Botta M Human DDX3 protein is a valuable target to develop broad  
28 spectrum antiviral agents. *Proc Natl Acad Sci U S A.* **2016**, *113*, 5388-5393.  
29  
30  
31  
32  
33 [20] Fazi R., Tintori C., Brai A., Selvaraj M. K., Bavagnoli L., Garbelli A., Maga G.,  
34 Botta M.. Homology model-based virtual screening for the identification of helicase  
35 human DDX3X inhibitors. *J. Chem. Inf. Model.* **2015**, *55*, 2443-2454.  
36  
37  
38  
39 [21] Yedavalli VS, Zhang N, Cai H, Zhang P, Starost MF, Hosmane RS, Jeang KT  
40 Ring expanded nucleoside analogues inhibit RNA helicase and intracellular human  
41 immunodeficiency virus type 1 replication, *J. Med. Chem.* **2008**, *51*, 5043-5051.  
42  
43  
44 [22] Yedavalli, V. S.; Neuveut, C.; Chi, Y. H.; Kleiman, L.; Jeang, K. T. Requirement  
45 of DDX3X DEAD box RNA helicase for HIV-1 Rev-RRE export function. *Cell.* **2004**,  
46 *119*, 381-392.  
47  
48  
49  
50  
51  
52  
53  
54  
55  
56  
57  
58  
59  
60

- 1  
2  
3 [23] Chaudhari SR, Mogurampelly S, Suryaprakash N. Engagement of CF<sub>3</sub> group in  
4 N-H···F-C hydrogen bond in the solution state: NMR spectroscopy and MD simulation  
5 studies, *J Phys Chem B*. **2013**;117, 1123-1129.  
6  
7  
8  
9  
10 [24] Linke S, Ellerbrok H, Niedrig M, Nitsche A, Pauli G. Detection of West Nile  
11 virus lineages 1 and 2 by real-time PCR. *J Virol Methods*. **2007**, 146, 355-358.  
12  
13  
14 [25] Bol GM, Vesuna F, Xie M, Zeng J, Aziz K, Gandhi N, Levine A, Irving A, Korz  
15 D, Tantravedi S, Heerma van Voss MR, Gabrielson K, Bordt EA, Polster BM, Cope L,  
16 van der Groep P, Kondaskar A, Rudek MA, Hosmane RS, van der Wall E, van Diest PJ,  
17 Tran PT, Raman V. Targeting DDX3 with a small molecule inhibitor for lung cancer  
18 therapy *EMBO Mol Med*. **2015**, 7, 648-669.  
19  
20  
21  
22  
23  
24  
25 [26] Verdonk, M. L.; Cole, J. C.; Hartshorn, M. J.; Murray, C. W.; Taylor, R. D.  
26 Improved protein-ligand docking using GOLD. *Proteins*, **2003**, 52, 609-623.  
27  
28  
29 [27] Cole, J. C.; Nissink, J. W. M.; Taylor, R. Protein-ligand docking and virtual  
30 screening with GOLD. In *Virtual Screening in Drug Discovery*, Eds. B. Shoichet, J.  
31 Alvarez, Taylor & Francis CRC Press, Boca Raton, Florida, USA, 2005.  
32  
33  
34  
35  
36 [28] PyMOL molecular graphics system, version 0.99, Schrödinger, LLC, New York,  
37 NY, USA, 2011.  
38  
39  
40  
41 [29] Maga, G., Falchi, F., Radi, M., Botta, L., Casaluce, G., Bernardini, M., Botta, M.  
42 Toward the discovery of novel anti-HIV drugs. Second-generation inhibitors of the  
43 cellular ATPase DDX3 with improved anti-HIV activity: synthesis, structure-activity  
44 relationship analysis, cytotoxicity studies, and target validation. *ChemMedChem*, **2011**, 6,  
45 1371-1389.  
46  
47  
48  
49  
50  
51  
52  
53  
54  
55  
56  
57  
58  
59  
60

## TABLE OF CONTENTS GRAPHIC

